Three-nucleon continuum reactions with chiral forces

H. Witała, J. Golak, R. Skibiński, K. Topolnicki, Jagiellonian University, Kraków

LENPIC collaboration

Content:

- 3N continuum reactions with standard forces
- Chiral NN potentials
- Applications of chiral NN potentials to elastic Nd scattering
- Chiral 3N-forces: results with N2LO 3NF’s
- Exploration of some N4LO 3NF contact terms

Theoretical description of 3N continuum (elastic nucleon-deuteron scattering and the deuteron breakup reaction) requires solution of the following Faddeev-type equation for $T|\phi_d\rangle$ state:

$$T\left|\phi_d\right\rangle = tP\left|\phi_d\right\rangle + \left(1+tG_0\right)V_4^{(1)}\left(1+P\right)\left|\phi_d\right\rangle$$
$$+ tPG_0T\left|\phi_d\right\rangle + \left(1+tG_0\right)V_4^{(1)}\left(1+P\right)G_0T\left|\phi_d\right\rangle,$$

where $\left|\phi_d\right\rangle \equiv \left|\varphi_d\right\rangle\left|\vec{q}_0\right\rangle$ is composed of the deuteron internal wave function and the state of the relative nucleon-deuteron motion.

The transition amplitude for elastic scaterring is given by:

$$\left\langle\phi_d'\left|U\right|\phi_d\right\rangle = \left\langle\phi_d'\left|PG_0^{-1}\right|\phi_d\right\rangle + \left\langle\phi_d'\left|V_4^{(1)}\left(1+P\right)\right|\phi_d\right\rangle$$
$$+\left\langle\phi_d'\left|PT\right|\phi_d\right\rangle + \left\langle\phi_d'\left|V_4^{(1)}\left(1+P\right)G_oT\right|\phi_d\right\rangle$$

for breakup :

$$\left\langle\phi_0\left|U_0\right|\phi_d\right\rangle = \left\langle\phi_0\left|\left(1+P\right)T\right|\phi_d\right\rangle$$

Few-Body Systems 16, 127–142 (1994)

Few-Body Systems

© Springer-Verlag 1994
Printed in Austria

Resolution of Discrepancy Between Backward Angle Cross-Section Data for Neutron-Deuteron Elastic Scattering

C. R. Howell[1], W. Tornow[1], H. R. Setze[1], R. T. Braun[1], D. E. Gonzalez Trotter[1], C. D. Roper[1], R. S. Pedroni[2,*], S. M. Grimes[2], C. E. Brient[2], N. Al-Niemi[2,**], F. C. Goeckner[2], and G. Mertens[3]

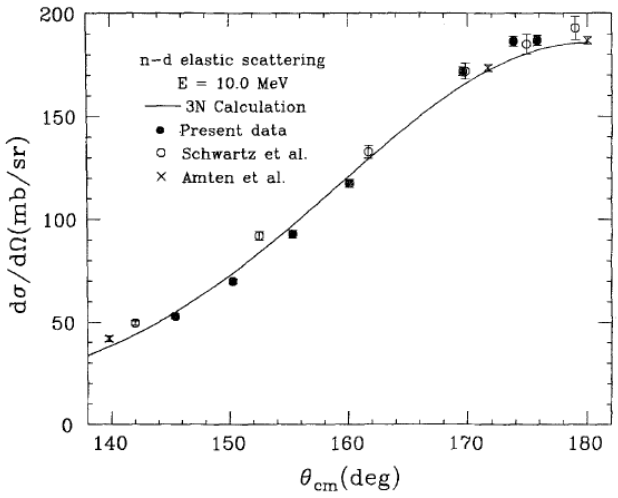

Fig. 13. Backward-angle $d\sigma(\theta)/d\Omega$ for *n-d* elastic scattering at 10 MeV. The data and curve are the same as in Fig. 2 with the addition of the present data

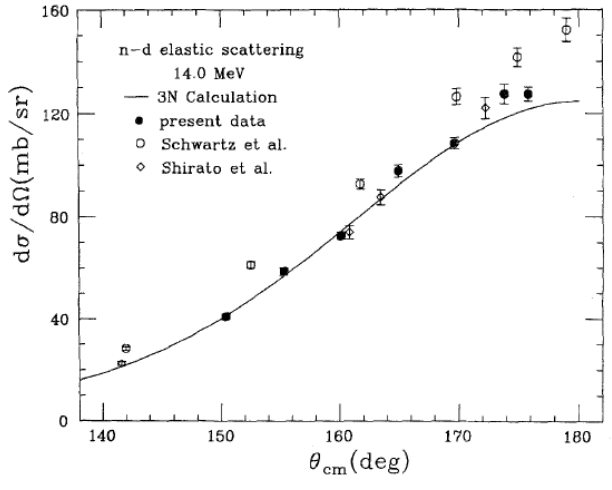

Fig. 14. Backward-angle $d\sigma(\theta)/d\Omega$ for *n-d* elastic scattering at 14 MeV. The data and curve are the same as in Fig. 3 with the addition of the present data and the exclusion of the data of Brüllmann et al. [13], which do not extend to backward angles

ELSEVIER

Physics Reports 274 (1996) 107–285

PHYSICS REPORTS

The three-nucleon continuum: achievements, challenges and applications

W. Glöckle[a], H. Witała[b], D. Hüber[a], H. Kamada[a,1], J. Golak[b]

[a] *Institut für theoretische Physik II, Ruhr-Universitat Bochum, D-44780 Bochum, Germany*

[b] *Institute of Physics, Jagellonian University, PL-30059 Cracow, Poland*

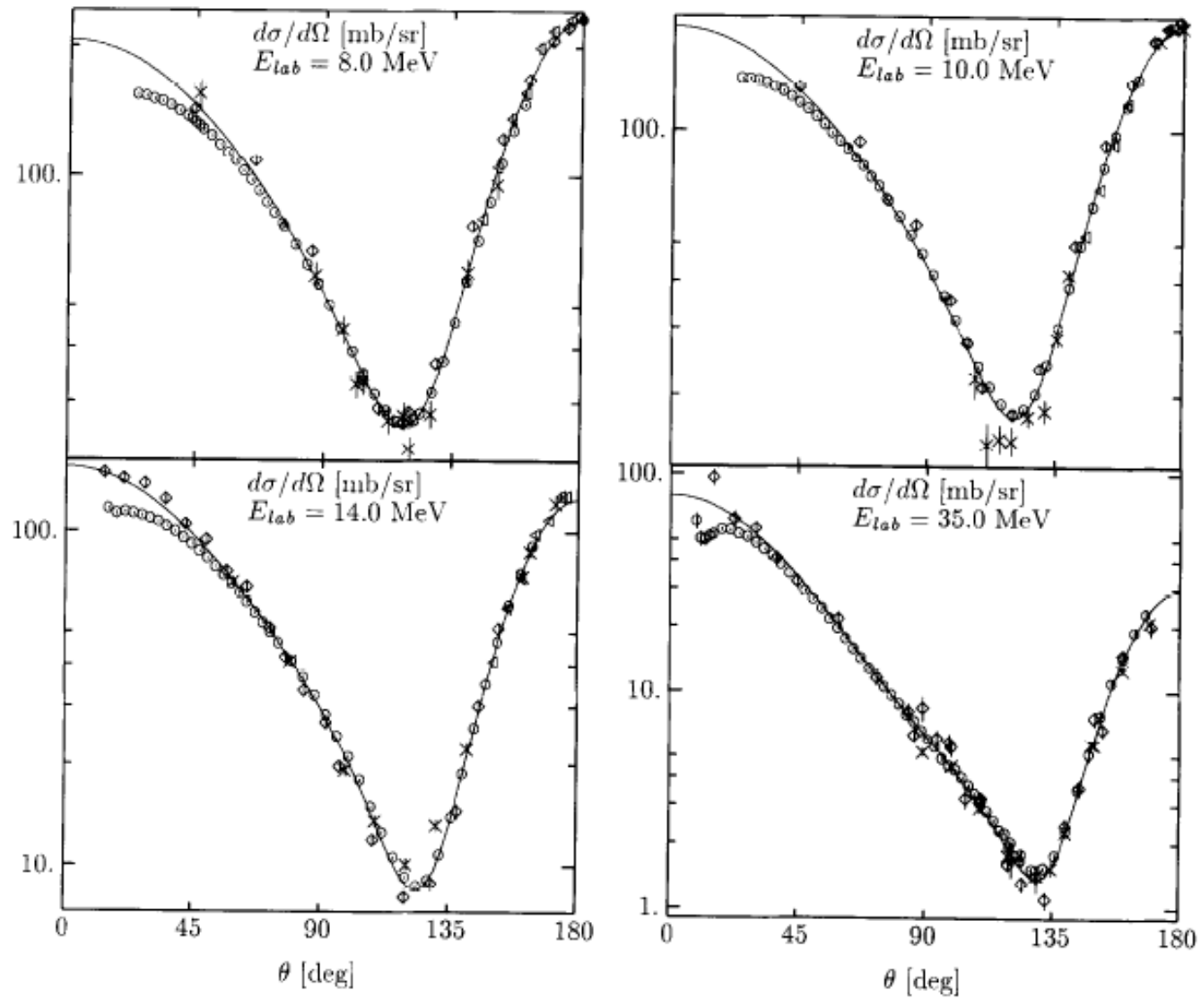

Fig. 7. Angular distributions for elastic Nd scattering. Comparison of pd and nd data. 8 MeV: nd data (◇) [431], (●) [252], (×) [436], (◁) [234]; pd data (○) [416]. 10 MeV: nd data (◇) (10.3 MeV) [431], (×) [24], (◁) [234]; pd data (○) [416]. 14 MeV: nd data (×) [440], (◁) [234], (◇) [47]; pd data (○) [416]. 35 MeV: nd data (×) [62], (◇) (36 MeV) [411]; pd data (○) [71]. The solid curve is the AV18 NN force prediction for 8, 10 and 14 MeV and the Nijm I NN force prediction for 35 MeV.

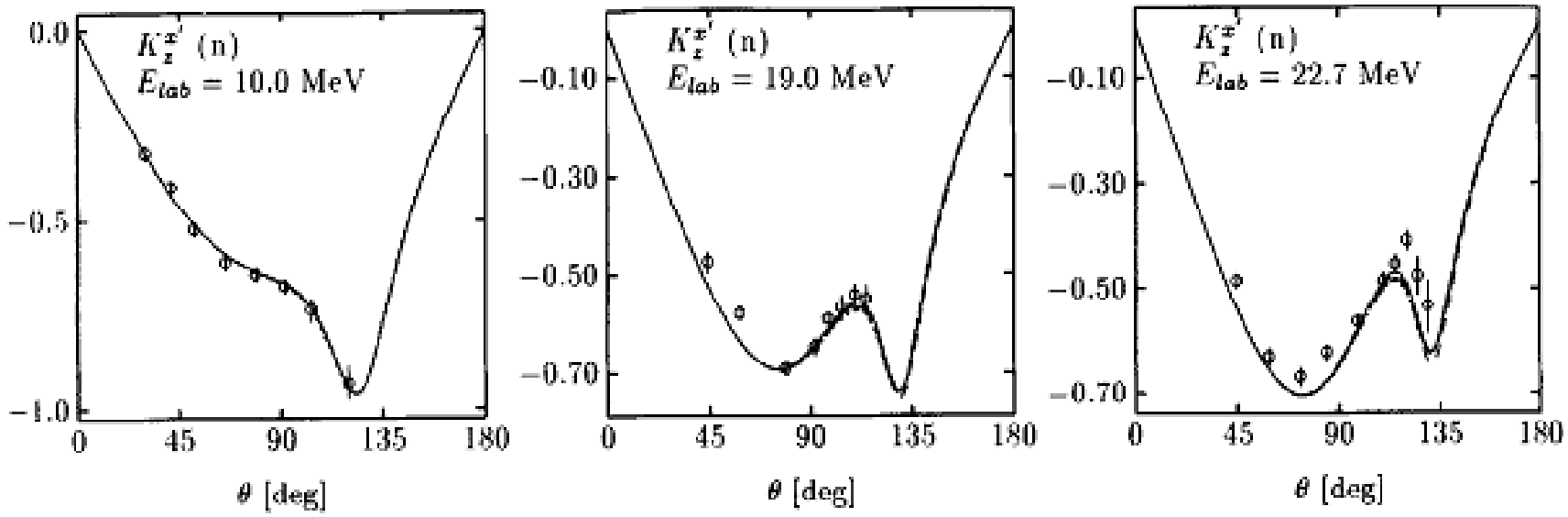

Fig. 22. The nucleon to nucleon spin transfer coefficient $K_z^{z'}$ for elastic Nd scattering. Comparison of data with NN force predictions. 10 MeV: pd data (○) [457]. 19 MeV: pd data (○) [474]. 22.7 MeV: pd data (○) [300,301,186]. The NN force predictions are (——) Nijm I, (– – –) Nijm II, (- - - - -) Nijm 93, and (·····) AV18.

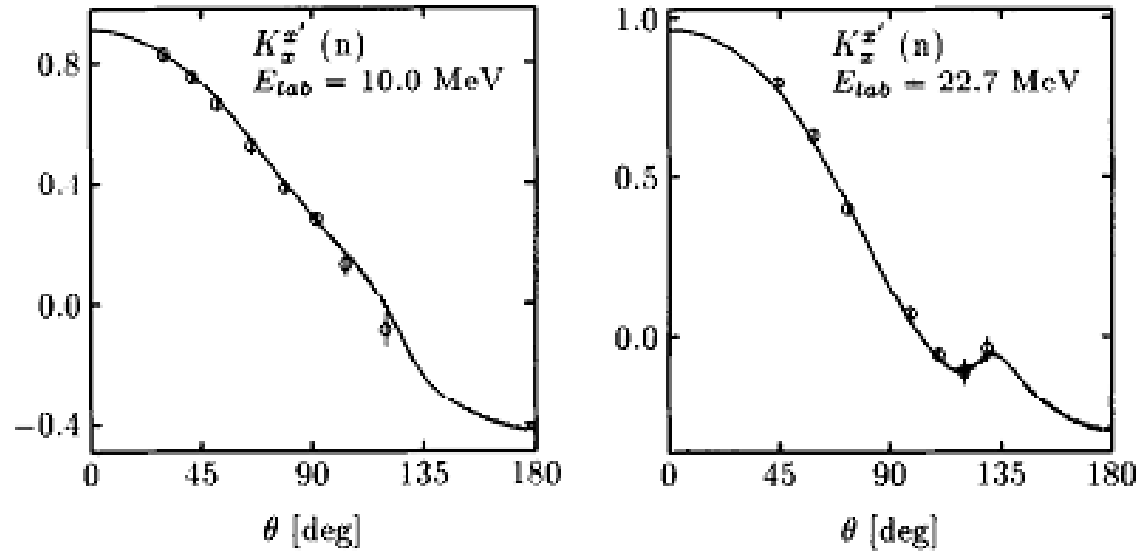

Fig. 23. The nucleon to nucleon spin transfer coefficient $K_x^{x'}$ for elastic Nd scattering. Comparison of data with NN force predictions. 10 MeV: pd data (○) [457]. 22.7 MeV: pd data (○) [300,301,186]. The NN force predictions are (——) Nijm I, (– – –) Nijm II, (- - - - -) Nijm 93, and (·····) AV18.

For elastic N+d scattering 3N force effects grow with energy !

H.Witała et al., PRL 81, 1183 (1998)

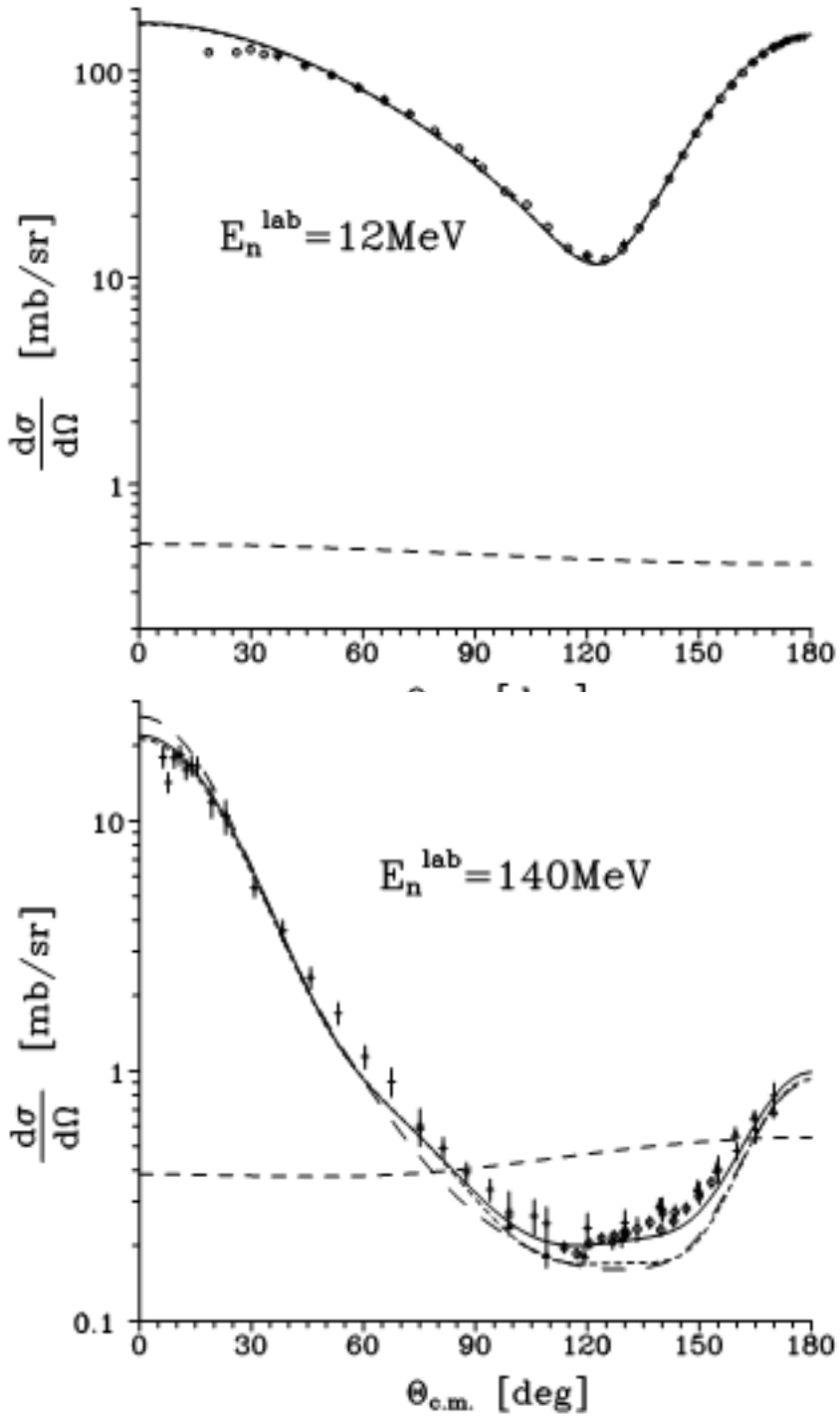

Higher energy discrepancies

Elastic scattering d(p,p)d

NN only (AV18, CD Bonn, Nijm1, Nijm2)

NN+3NF TM99

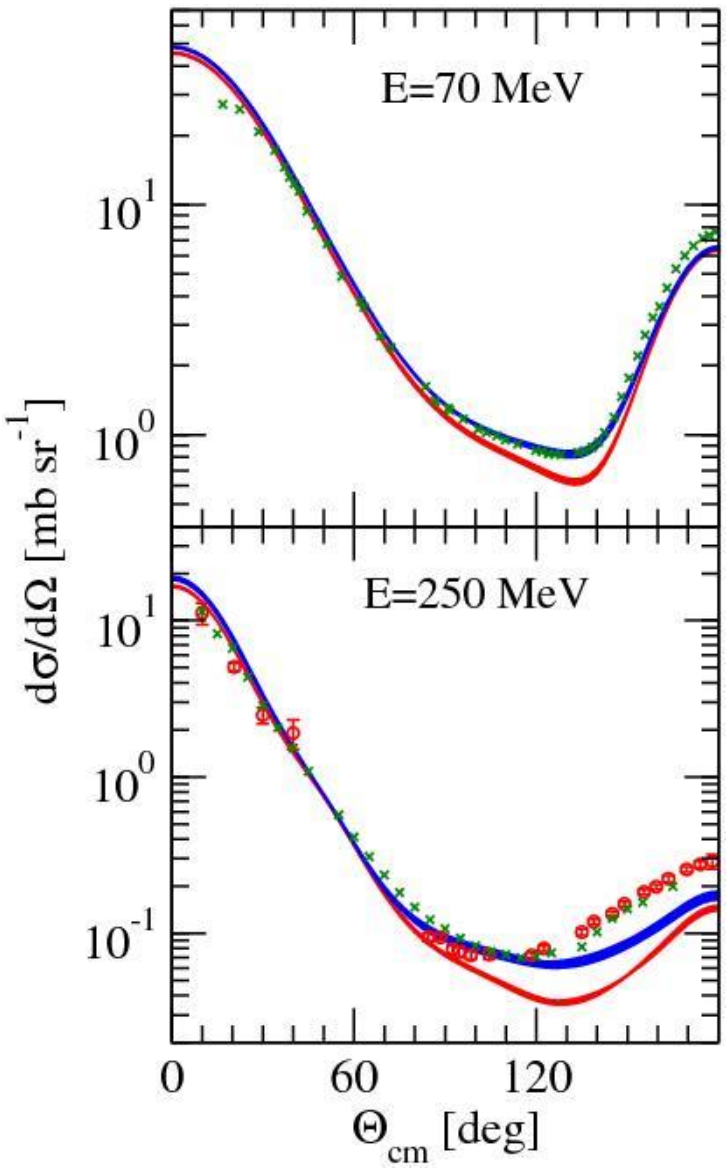

data 70: K.Sekiguchi et al., PR C65, 034003 (2002)

data 250:
x nd – Y.Maeda et al., PR C76, 014004 (2007)
o pd – K.Hatanaka et al., PR C 66, 044002 (2002)

Total nd cross section: (W.P.Abfalterer et al. PRL 81(1998)57)

- **up to ~ 50 MeV good agreement with predictions based on 2N forces**
- **adding 3NF provides explanation of the disagreement up to ~ 150 MeV**
- **at even larger energies a clear disagreement which increases with energy**

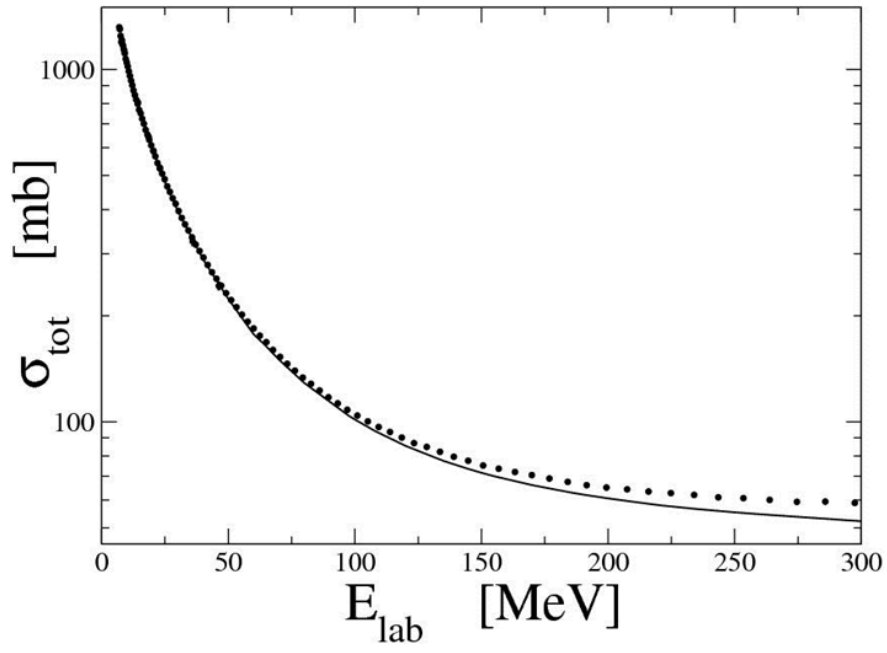

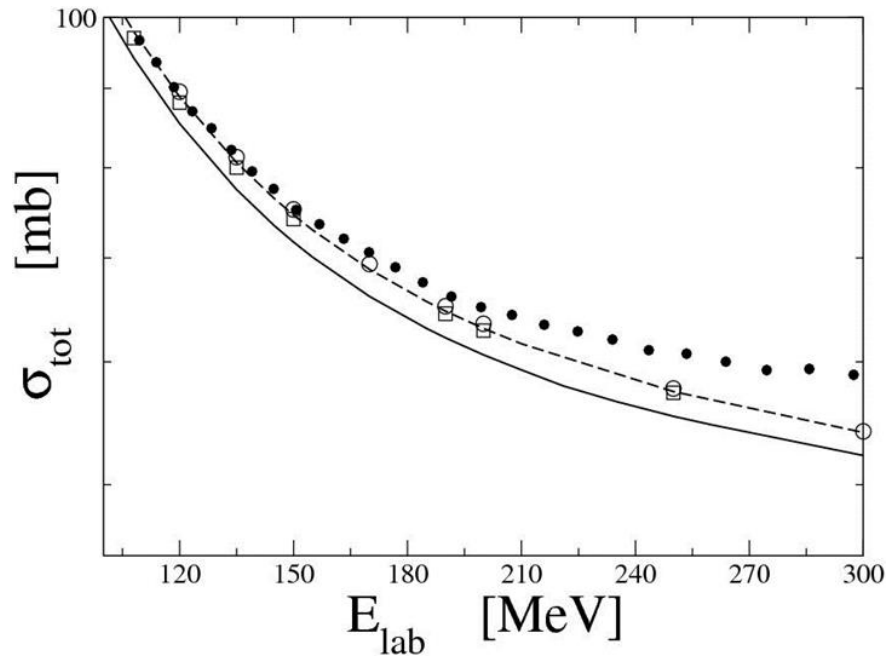

E=135 MeV

K.Sekiguchi et al.,PRC70, 014001 (2004)

d(p,p)d

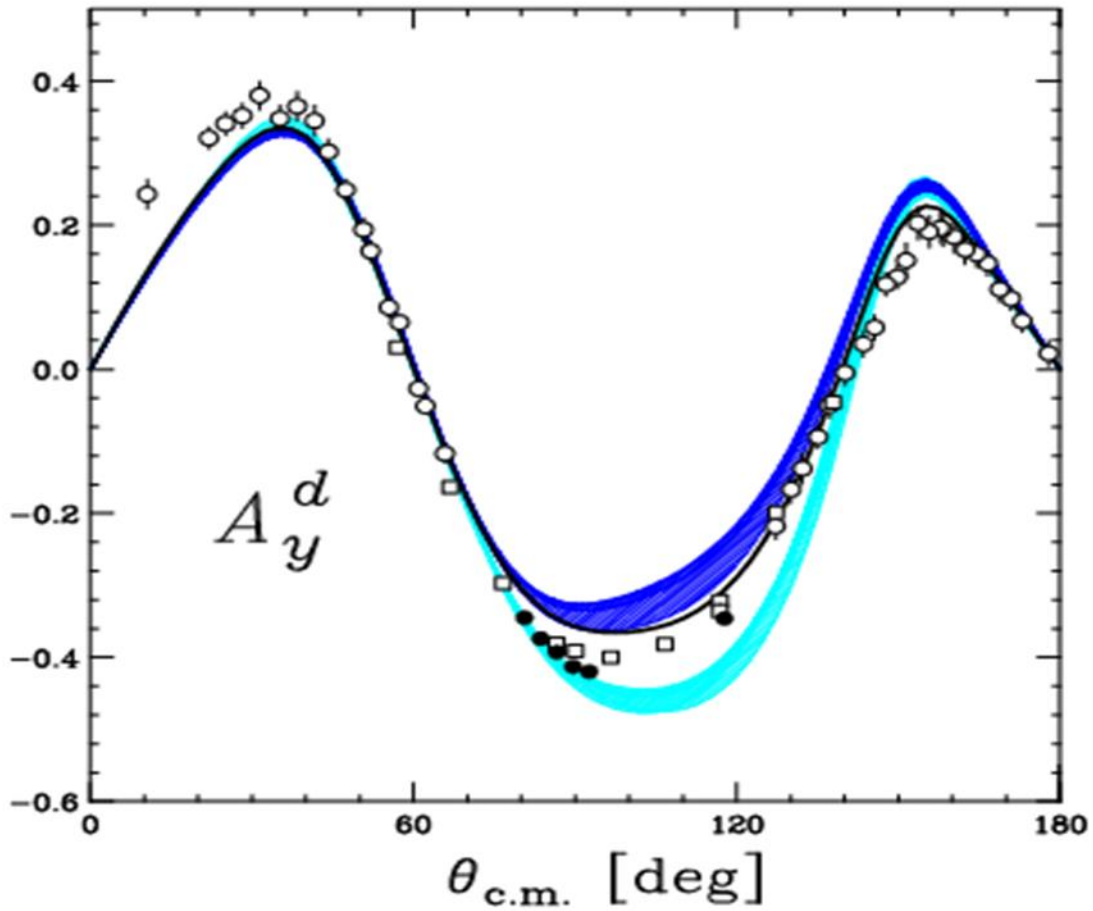

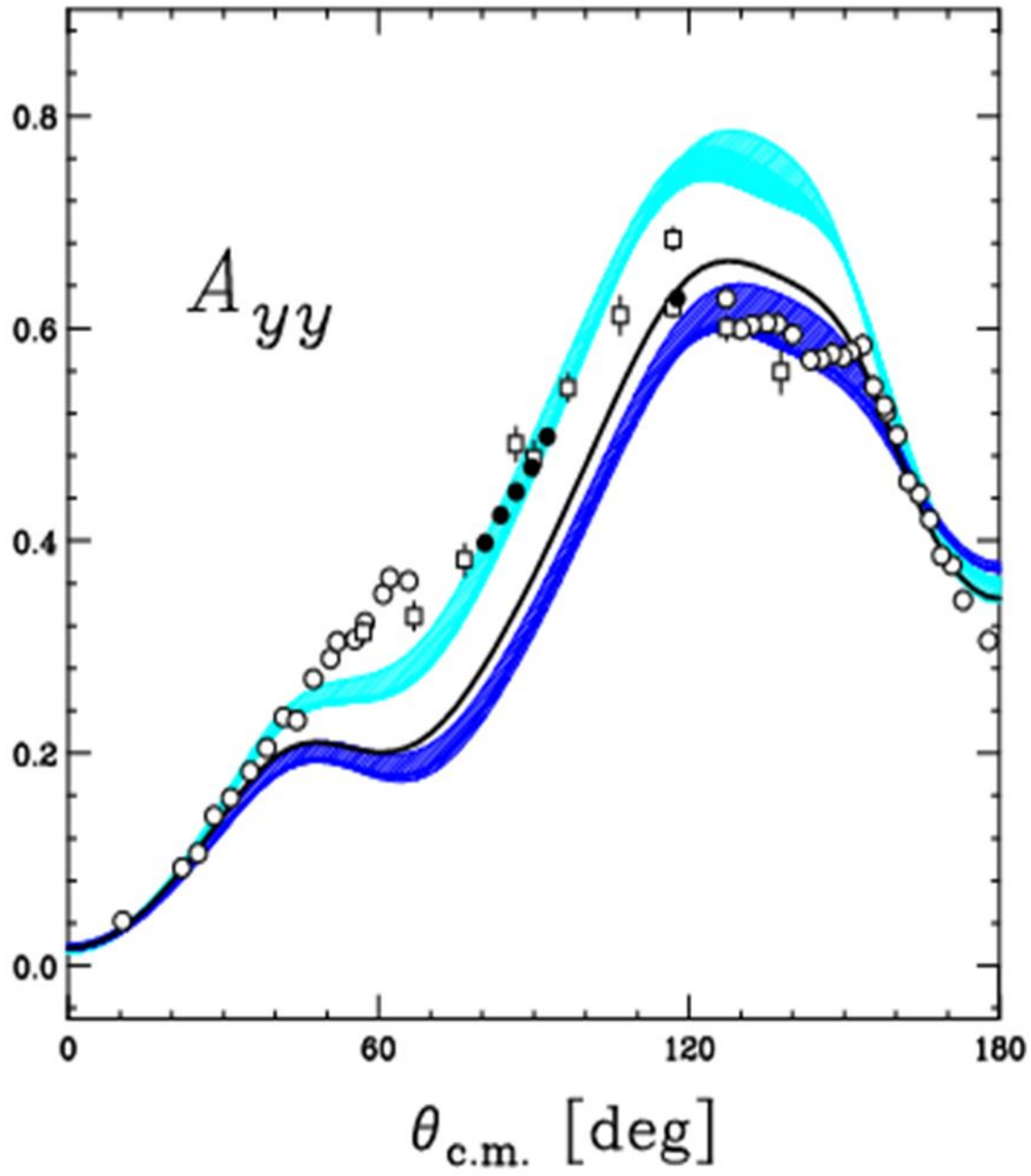

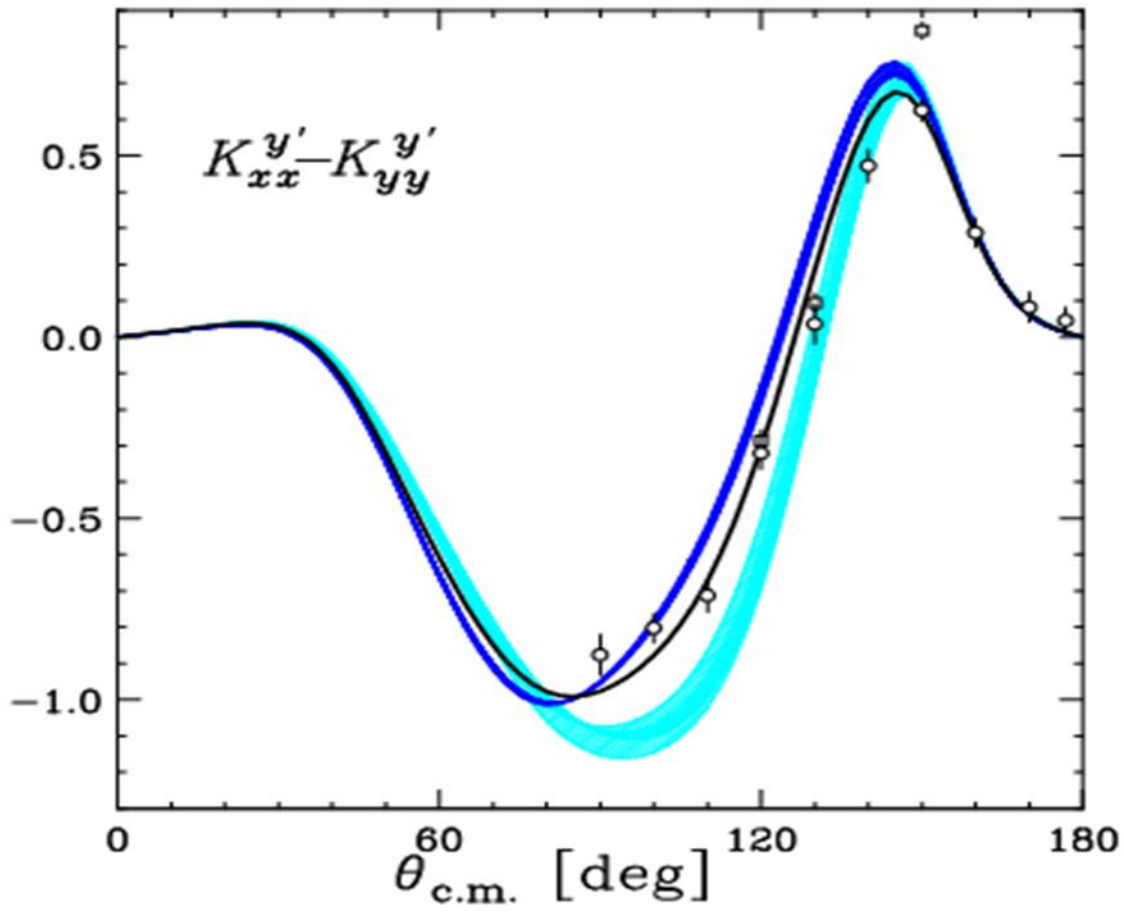

light shaded band: AV18, CDBonn, Nijm1 and Nijm2
blue band: standard NN + TM99 3NF

black solid line: AV18+UrbanaIX 3NF

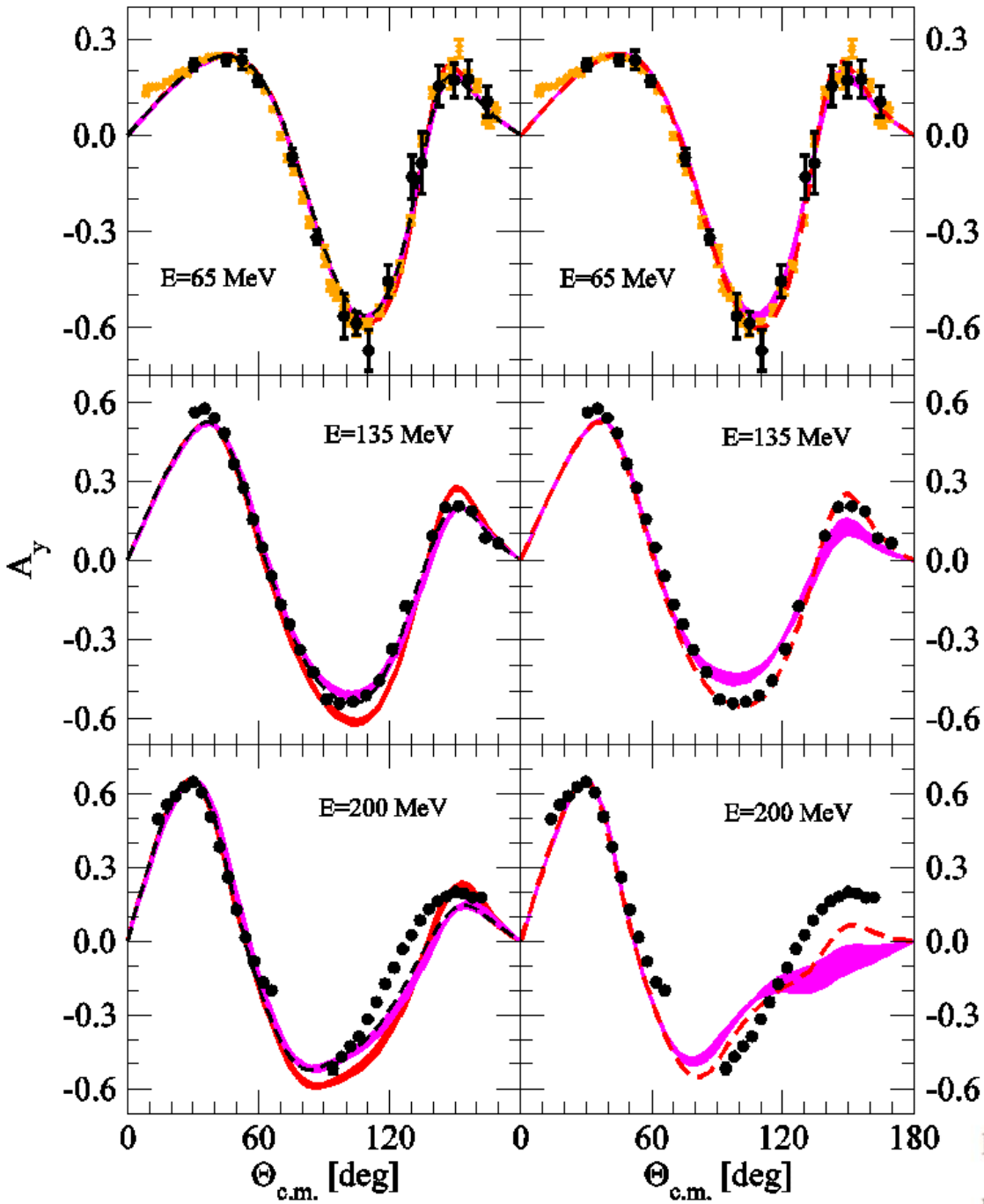

FIG. 5: (Color online) The nd elastic scattering neutron analyzing power A_y at the incoming neutron laboratory energies $E = 65, 135$, and 200 MeV. In the left column predictions of (semi-)phenomenological NN potentials alone or combined with the TM99 and the Urbana IX 3NF's are shown while in the right column predictions of the N^{4}LO SCS NN potential with the regulator $R = 0.9$ fm alone or combined with the N^{2}LO 3NF for four pairs of strengths c_D and c_E values of the contact terms. For explanation of bands and lines see Fig. 4. At $E = 65$ MeV the (black) dots are nd data from Ref. [39] and the (orange) x-ces are pd data from Ref. [24]. At $E = 135$ MeV the (black) dots are pd data from Ref. [40]. At $E = 200$ MeV the (black) dots are pd data from Ref. [41].

- **relativistic effects are not responsible for large discrepancies in elastic Nd scattering**

- **very probably those discrepancies come from neglection of short-range 3NF components, which become active at higher energies**
- **such short-range 3NF's are in the meson-exchange picture given by π-ρ and ρ-ρ exchanges and in χPT comes a lot of short-range contributions in N^3LO order of chiral expansion (without free parameters)**

Challenge: apply NN and 3NF's derived consistently in the framework of the chiral perturbation theory

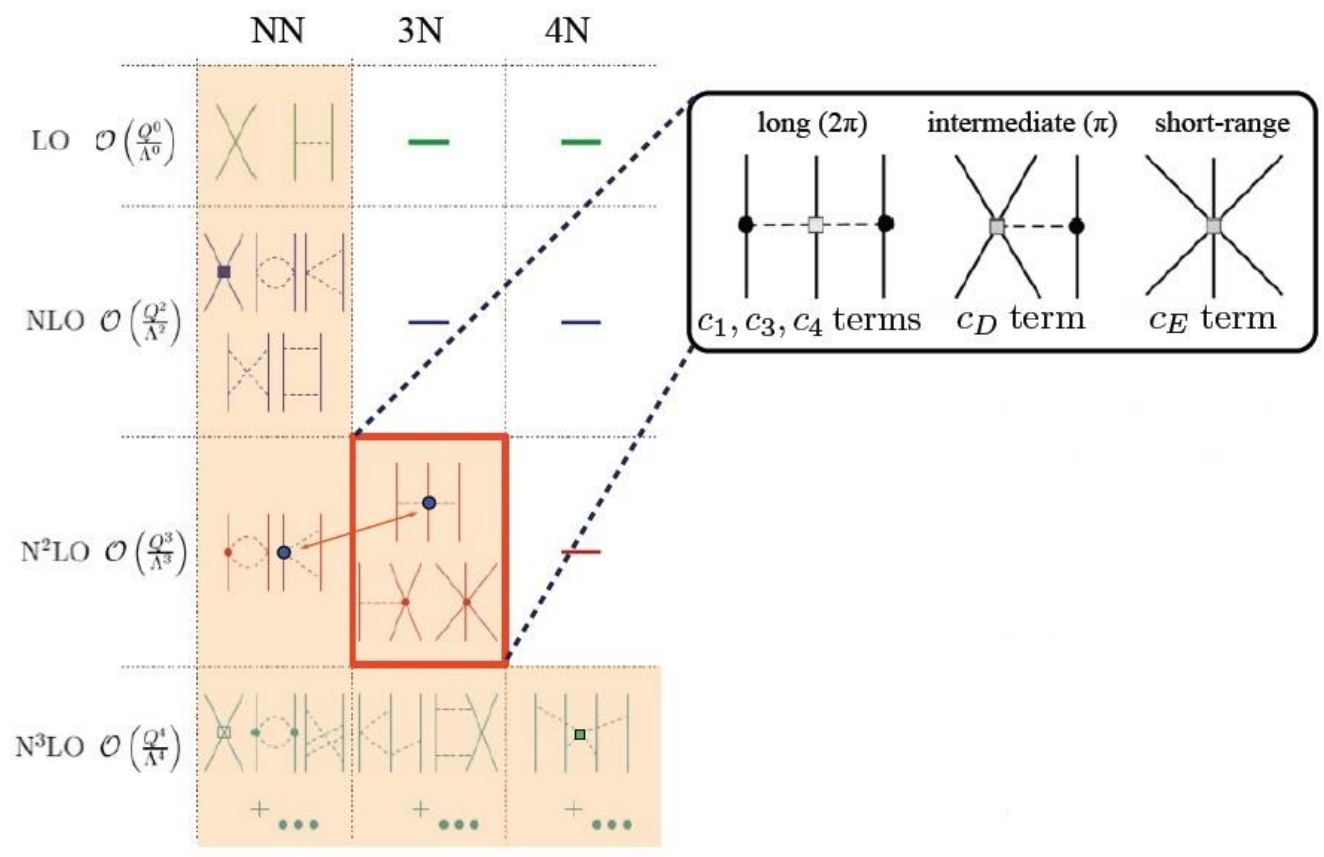

Chiral EFT for nuclear forces

perturbation in $(Q/\Lambda)^\nu$

LENPIC (Low Energy Nuclear Physics International Collaboration): to understand nuclear structure and reactions with chiral forces

LENPIC

TECHNISCHE UNIVERSITÄT DARMSTADT
Sven Binder, Angelo Calci, Kai Hebeler, Joachim Langhammer, Robert Roth

RUB
Evgeny Epelbaum, Hermann Krebs

JÜLICH FORSCHUNGSZENTRUM
Susanna Liebig, David Minossi, Andreas Nogga

IOWA STATE UNIVERSITY
Pieter Maris, Hugh Potter, James Vary

THE OHIO STATE UNIVERSITY
Richard J. Furnstahl,

IPN ORSAY
Veronique Bernard

JAGIELLONIAN UNIVERSITY IN KRAKOW
Jacek Golak, Roman Skibiński, Kacper Topolnicki, Henryk Witała

Kyutech
Hiroyuki Kamada

universitätbonn
Ulf-G.Meißner

Few remarks on chiral forces:

- In order to reproduce properly 2N data up to about 250 MeV N3LO order of chiral expansion is required
  - About 10 years ago: NN interaction up to N3LO, 3NF interaction up to N2LO (N3LO used in preliminary calculations at low energies)
  - nonlocal momentum space regularization has been applied:

    V $\rightarrow$ f(p',Λ) V(p',p) f(p,Λ) with $f(p,\Lambda) = e^{-p^6/\Lambda^6}$

    $V^4 \rightarrow$ f(p',q',Λ) V^4(p',q',p',q) f(p,q,Λ) with $f(p,q,\Lambda) = e^{-(p^2+0.75q^2)^3/\Lambda^6}$

    what leads to finite cut-off artefacts (problems when applied to higher energy Nd scattering)

- New, improved chiral force, presented by Bochum-Bonn group in 2014 (SCS):
  - E. Epelbaum, H. Krebs, U.-G. Meißner, Eur. Phys. J. A51 (2015) 3,26 – up to N3LO
  - E. Epelbaum, H. Krebs, U.-G. Meißner arXiv:1412.4623 [nucl-th] – up to N4LO
  - Local regularization in the coordinate space $V_{lr}(\mathbf{r}) \rightarrow V_{lr}(\mathbf{r})f(\mathbf{r})$ with $f(r) = (1-e^{-r^2/R^2})^n$
  - R=0.8–1.2 fm what corresponds to Λ=330-500 MeV
  - Such regularization preserves more long-range OPE and TPE physics
  - All LECs in the long-range part are taken from pion-nucleon scattering without fine tuning
  - Very good description of the deuteron properties, phase shifts etc.

Semilocal momentum-space regularized chiral two-nucleon potentials up to fifth order

P. Reinert,[1,*] H. Krebs,[1,†] and E. Epelbaum[1,‡]

[1]*Institut für Theoretische Physik II, Ruhr-Universität Bochum, D-44780 Bochum, Germany*

We introduce new semilocal two-nucleon potentials up to fifth order in the chiral expansion. We employ a simple regularization approach for the pion-exchange contributions which (i) maintains the long-range part of the interaction, (ii) is implemented in momentum space and (iii) can be straightforwardly applied to regularize many-body forces and current operators. We discuss in detail the two-nucleon contact interactions at fourth order and demonstrate that three terms out of fifteen used in previous calculations can be eliminated via suitably chosen unitary transformations. The removal of the redundant contact terms results in a drastic simplification of the fits to scattering data and leads to interactions which are much softer (i.e. more perturbative) than our recent semilocal coordinate-space regularized potentials. Using the pion-nucleon low-energy constants from matching pion-nucleon Roy-Steiner equations to chiral perturbation theory, we perform a comprehensive analysis of nucleon-nucleon scattering and the deuteron properties up to fifth chiral order and study the impact of the leading F-wave two-nucleon contact interactions which appear at sixth order. The resulting chiral potentials lead to an outstanding description of the proton-proton and neutron-proton scattering data from the self-consistent Granada-2013 database below the pion production threshold, which is significantly better than for any other chiral potential. For the first time, the chiral potentials match in precision and even outperform the available high-precision phenomenological potentials, while the number of adjustable parameters is, at the same time, reduced by about $\sim 40\%$. Last but not least, we perform a detailed error analysis and, in particular, quantify for the first time the statistical uncertainties of the fourth- and the considered sixth-order contact interactions.

SMS:

- local regularization of long-range forces in momentum space
- regularization is achieved by replacing the Feynman propagators for pions, exchanged between different nucleons, by the spectral integrals with spectra function chosen to ensure that the static pion propagators get regularized

$$\int_0^\infty \mathrm{d}\mu^2 \frac{\rho(\mu^2)}{\vec{l}^{\,2}+\mu^2} \to \frac{F(\vec{l}^{\,2})}{\vec{l}^{\,2}+M_\pi^2}$$

The form factor $F(l^2)$ is choosen to be of a Gausian type with Λ cutoff $\quad F(\vec{l}^{\,2}) = e^{-\frac{\vec{l}^{\,2}+M_\pi^2}{\Lambda^2}}$

Estimation of theoretical uncertainties (E.Epelbaum et al., arXiv:1412.4623 [nucl-th], arXiv:1505.07218 [nucl.th]):

X(p) - observable and $X^{(i)}, i = 0, 2, 3, \ldots$ prediction at order $Q^{(i)}$ in the chiral expansion

Order-$Q^{(i)}$ correction :

$$\Delta X^{(2)} = X^{(2)} - X^{(0)}$$
$$\Delta X^{(i)} = X^{(i)} - X^{(i-1)} \quad i \geq 3$$

The chiral expansion for X takes the form:

$X^{(i)} = X^{(0)} + \Delta X^{(2)} + \ldots + \Delta X^{(i)}$ Size of corrections is expected to be $\Delta X^{(i)} = O(Q^{(i)} X^{(0)})$

Quantitative estimates of the theoretical uncertainty $\delta X^{(i)}$ of the prediction $X^{(i)}$ is made using the expected and actual sizes of higher-order contributions:

$$\delta X^{(0)} = Q^2 \left| X^{(0)} \right|$$
$$\delta X^{(2)} = \max(Q^3 \left| X^{(0)} \right|, Q^1 \left| \Delta X^{(2)} \right|)$$

$$i \geq 3: \quad \delta X^{(i)} = \max(Q^{i+1} \left| X^{(0)} \right|, Q^{i-1} \left| \Delta X^{(2)} \right|, Q^{i-2} \left| \Delta X^{(3)} \right|)$$
$$\delta X^{(2)} \geq Q \delta X^{(0)}, \ \delta X^{(i \geq 3)} \geq Q \delta X^{(i-1)}$$

$Q = \max(p/\Lambda_b, m_\pi / \Lambda_b)$ with $\Lambda_b = 600, 500$ and 400 MeV

for regulator R=0.8-1.0 fm, R=1.1 fm and R=1.2 fm, respectively.

- NN developed up to N4LO: E.Epelbaum et al. arXiv:1412.4623 [nucl-th]
- Novel way of quantifying the theoetical uncertainty due to the truncation of the chiral expansion: E.Epelbaum et al. arXiv:1412.0142 [nucl-th]

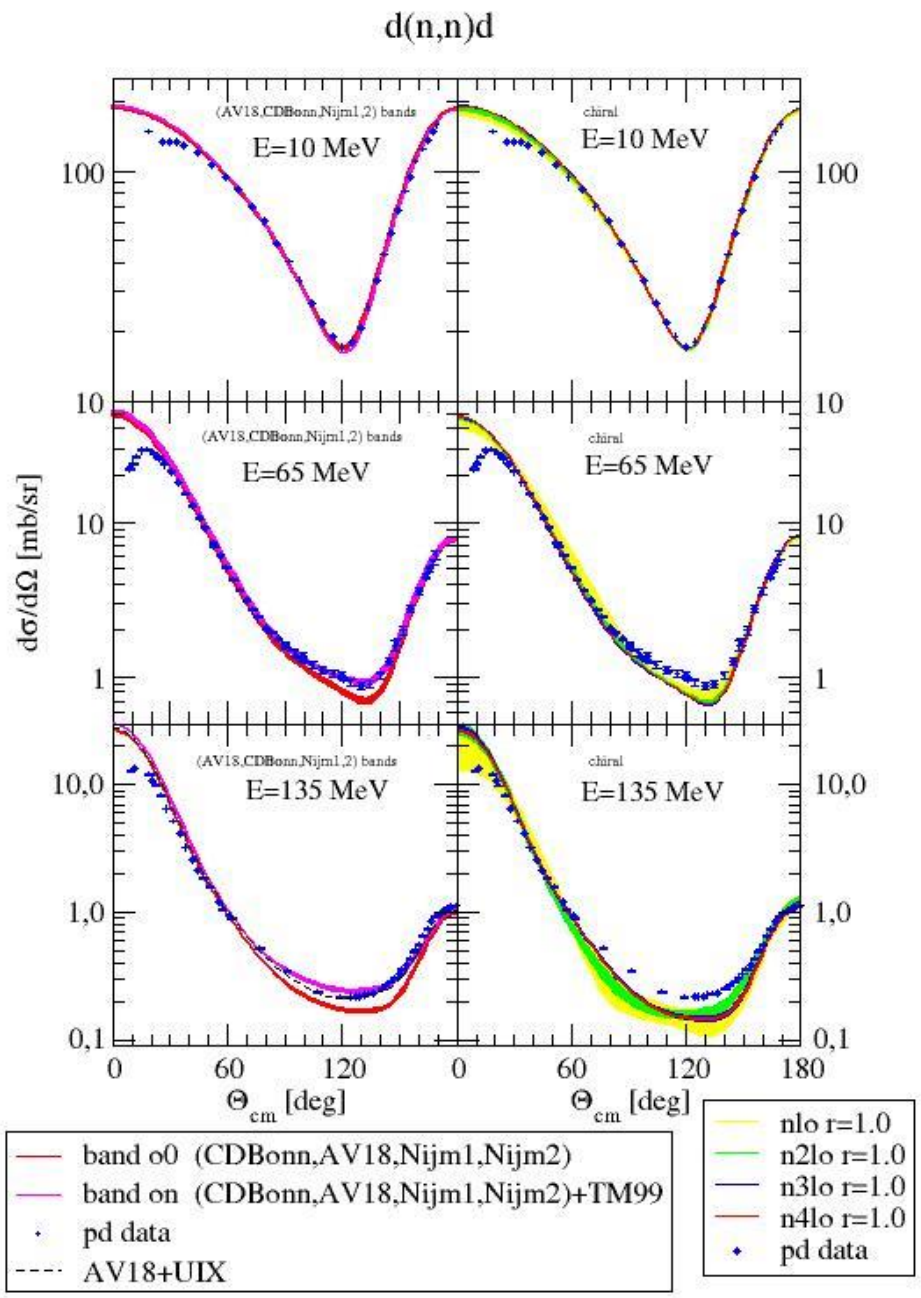

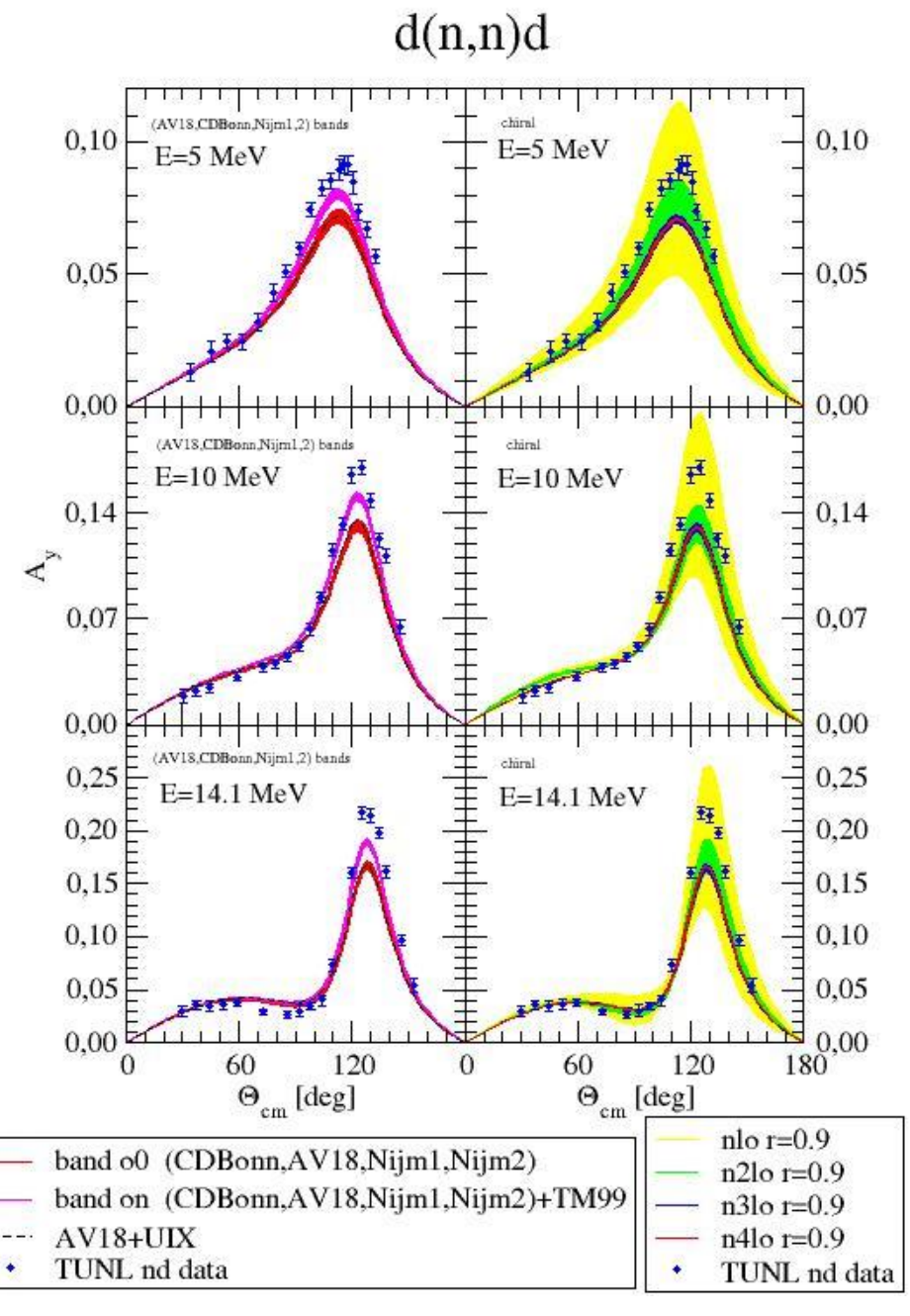

- Theoretical uncertainty grows with energy and decreases with increasing order: one thus expects precise predictions starting from N3LO
- For many observables the results at N2LO and higher orders differ from data well outside the range of quantified observables, thus providing a clear evidence for missing three-nucleon forces

Exclusive breakup reaction: symmetric space-star configuration

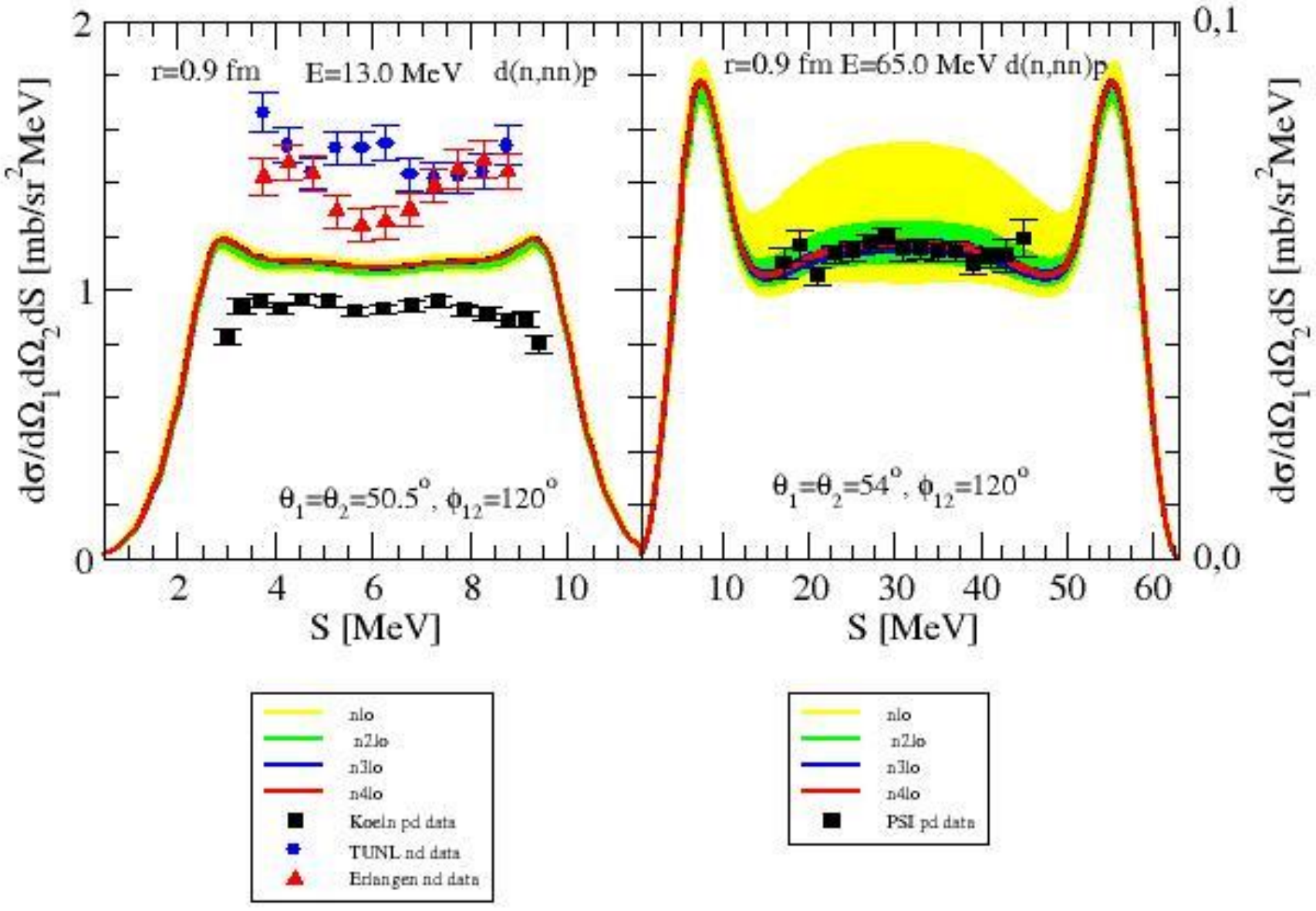

Big challenge: application of full chiral force: NN + 3NF

Chiral 3N potential in N^{2}LO order:

E.Epelbaum, Prog.Part.Nucl.Phys. 57, 654 (2006)

$$V_{123} = V_{2\pi}^{(3)} + V_{1\pi,cont}^{(3)} + V_{cont}^{(3)}$$

$$V_{2\pi}^{(3)} = \sum_{i\neq j\neq k} \frac{1}{2}\left(\frac{g_A}{2F_\pi}\right)^2 \frac{(\vec{\sigma}_i \circ \vec{q}_i)(\vec{\sigma}_j \circ \vec{q}_j)}{(\vec{q}_i^{\,2} + M_\pi^2)(\vec{q}_j^{\,2} + M_\pi^2)} F_{ijk}^{\alpha\beta} \tau_i^\alpha \tau_j^\beta$$

$$\vec{q}_i \equiv \vec{p}_i\,' - \vec{p}_i$$

$$F_{ijk}^{\alpha\beta} = \delta^{\alpha\beta}\left[-\frac{4c_1 M_\pi^2}{F_\pi^2} + \frac{2c_3}{F_\pi^2}\vec{q}_i \circ \vec{q}_j\right] + \sum_\gamma \frac{c_4}{F_\pi^2}\varepsilon^{\alpha\beta\gamma}\tau_k^\gamma \vec{\sigma}_k \circ \left[\vec{q}_i \times \vec{q}_j\right]$$

$$V_{1\pi,cont}^{(3)} = -\sum_{i\neq j\neq k} \frac{g_A}{8F_\pi^2} D \frac{\vec{\sigma}_j \circ \vec{q}_j}{\vec{q}_j^{\,2} + M_\pi^2}\left(\vec{\tau}_i \circ \vec{\tau}_j\right)\left(\vec{\sigma}_i \circ \vec{q}_j\right)$$

$$V_{cont}^{(3)} = \frac{1}{2}\sum_{j\neq k} E\left(\vec{\tau}_j \circ \vec{\tau}_k\right)$$

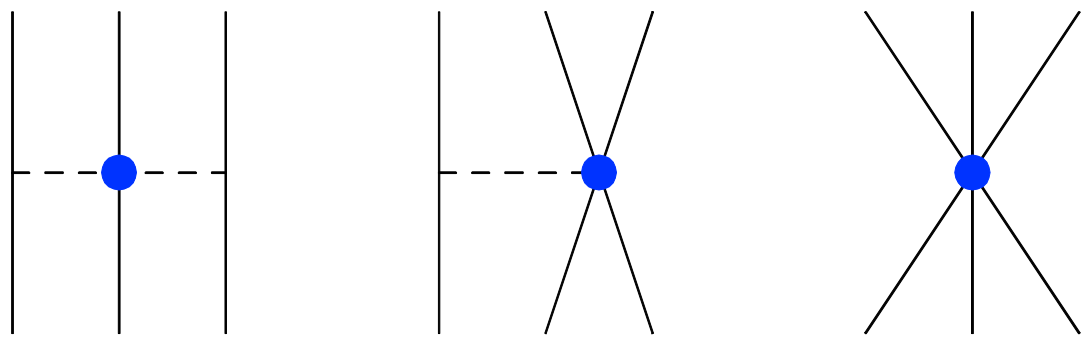

Two free parameters : D i E

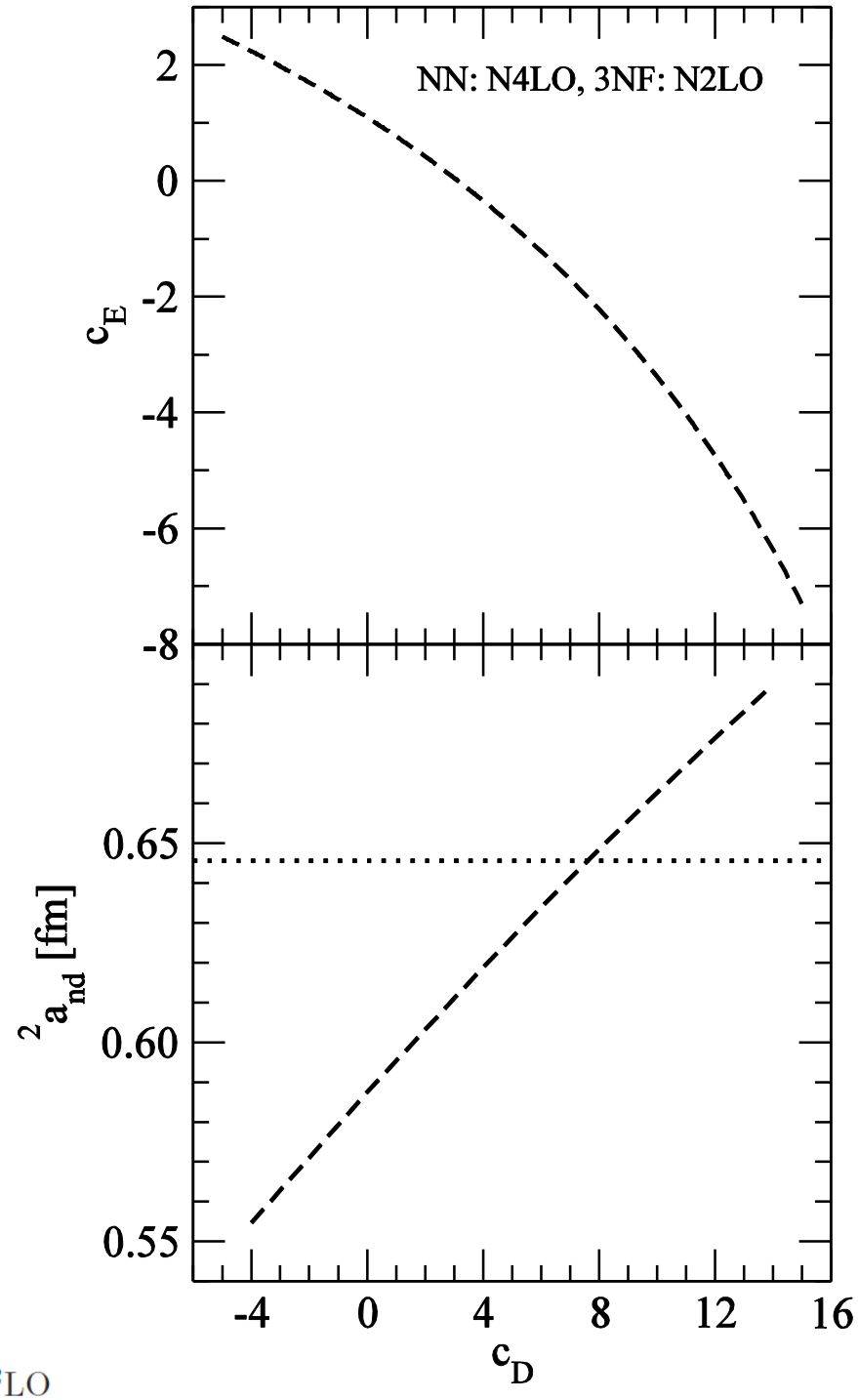

FIG. 1: (Color online) Upper part: a correlation function for the strengths c_D and c_E of the N^{2}LO 3NF contact terms. The ^{3}H experimental binding energy is reproduced by combining of the N^{4}LO SCS chiral NN potential and a N^{2}LO 3NF with strengths c_D and c_E lying on the dashed (black) line. In the lower part the corresponding doublet nd scattering lengths are shown by the dashed (black) line. The dotted (black) line is the experimental value $^2a_{nd}^{exp} = 0.645(7)$ fm [33].

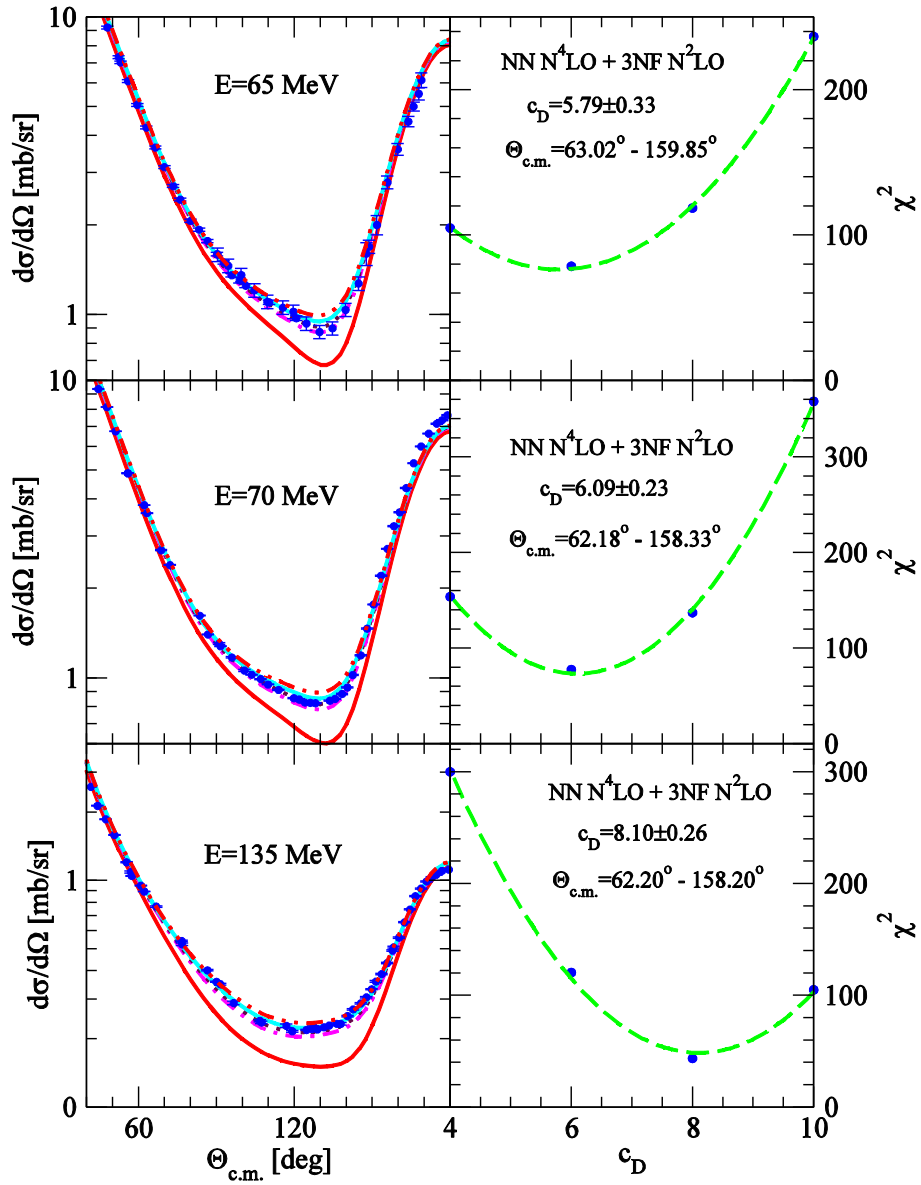

FIG. 2: (Color online) The nd elastic scattering cross section at the incoming neutron laboratory energies $E = 65, 70$, and 135 MeV. In the left part the solid (red) lines are predictions of the N^{4}LO SCS NN potential with the regulator $R = 0.9$ fm. Combining that NN potential with N^{2}LO 3NF with four different strengths c_D and c_E of the contact terms from the corelation line of Fig.1 leads to results obtained with different sets of (c_D, c_E) values and represented by different lines: dashed-dotted (magenta) (4.0,−0.270), dotted (maroon) (6.0,−1.094), solid (cyan) (8.0,−2.032), and double-dotted-dashed (red) (10.0,−3.108). The (blue) circles are pd data from Ref. [24] at $E = 65$ MeV, from Ref. [25] at $E = 70$ MeV, and from Ref. [25] at $E = 135$ MeV. In the right part the χ^2 fits to the experimental data, in angular region indicated at each energy, based of on these four pairs of (c_D, c_E) values, are shown by dashed (red) line together with the resulting optimal value of the strength c_D.

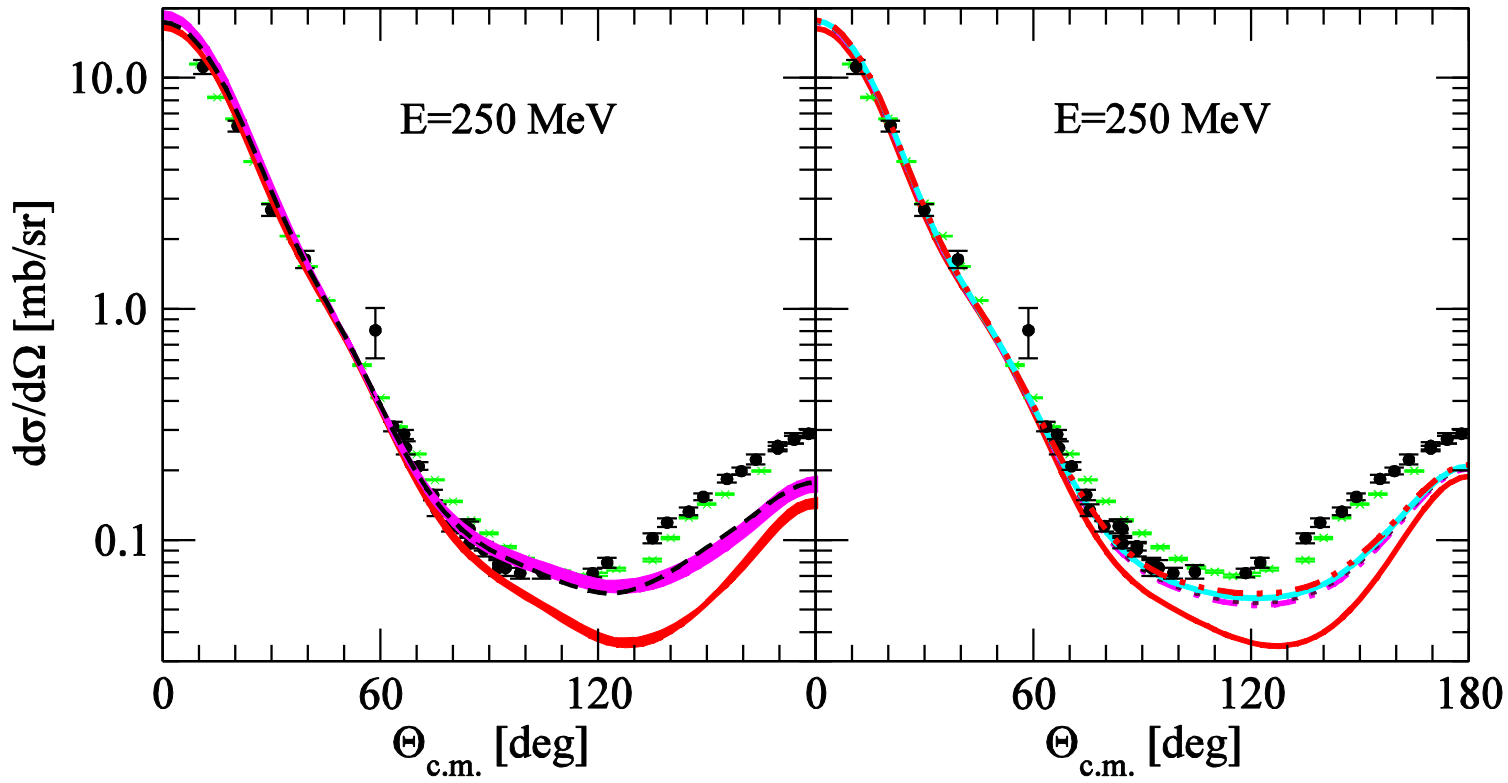

FIG. 3: (Color online) The nd elastic scattering cross section at the incoming neutron laboratory energy $E = 250$ MeV. In the left part predictions of (semi-)phenomenological NN potentials (AV18, CD Bonn, Nijm1 and Nijm2) are shown by dark (red) band. Results obtained when they are combined with the TM99 3NF are shown by a light (magenta) band. The dashed (black) line is the result of combination of the AV18 potential with the Urbana IX 3NF. In the right part the different lines are predictions of the N^{4}LO SCS NN potential with the regulator $R = 0.9$ fm alone or combined with N^{2}LO 3NF for four different strengths c_D and c_E of the contact terms. For explanation of these lines see Fig. 2. In left and right parts the (black) dots are pd data from Ref. [34] and (green) x-ces are nd data from Ref. [35].

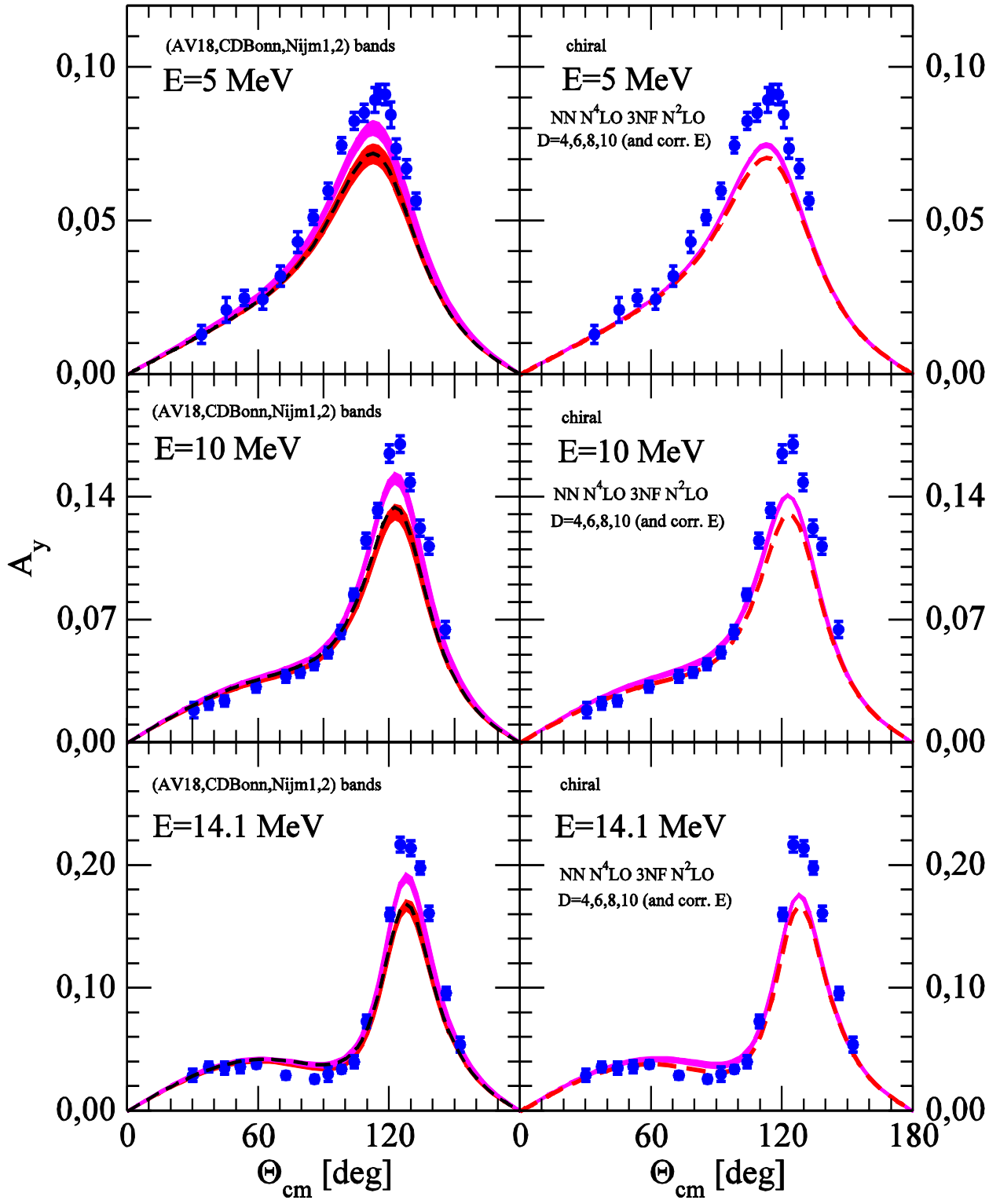

- small effects of N2LO 3N force
- effects are practically independent on D (E) values used
- will 3N force explain A_y puzzle (N3LO 3NF) ?
- alternative: wrong low energy NN phase-shifts (in P-waves)

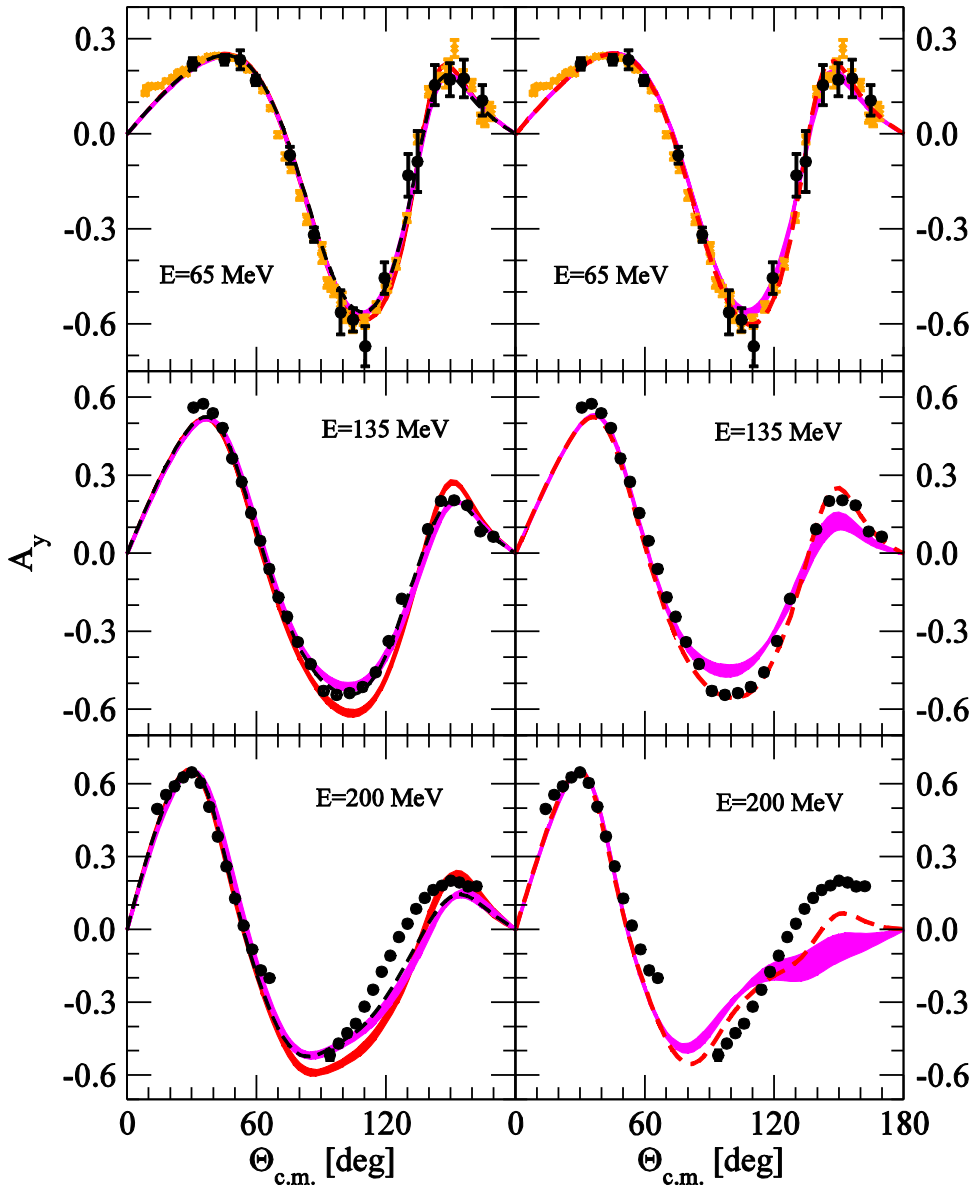

FIG. 5: (Color online) The nd elastic scattering neutron analyzing power A_y at the incoming neutron laboratory energies $E = 65, 135$, and 200 MeV. In the left column predictions of (semi-)phenomenological NN potentials alone or combined with the TM99 and the Urbana IX 3NF's are shown while in the right column predictions of the N^{4}LO SCS NN potential with the regulator $R = 0.9$ fm alone or combined with the N^{2}LO 3NF for four pairs of strengths c_D and c_E values of the contact terms. For explanation of bands and lines see Fig. 4. At $E = 65$ MeV the (black) dots are nd data from Ref. [39] and the (orange) x-ces are pd data from Ref. [24]. At $E = 135$ MeV the (black) dots are pd data from Ref. [40]. At $E = 200$ MeV the (black) dots are pd data from Ref. [41].

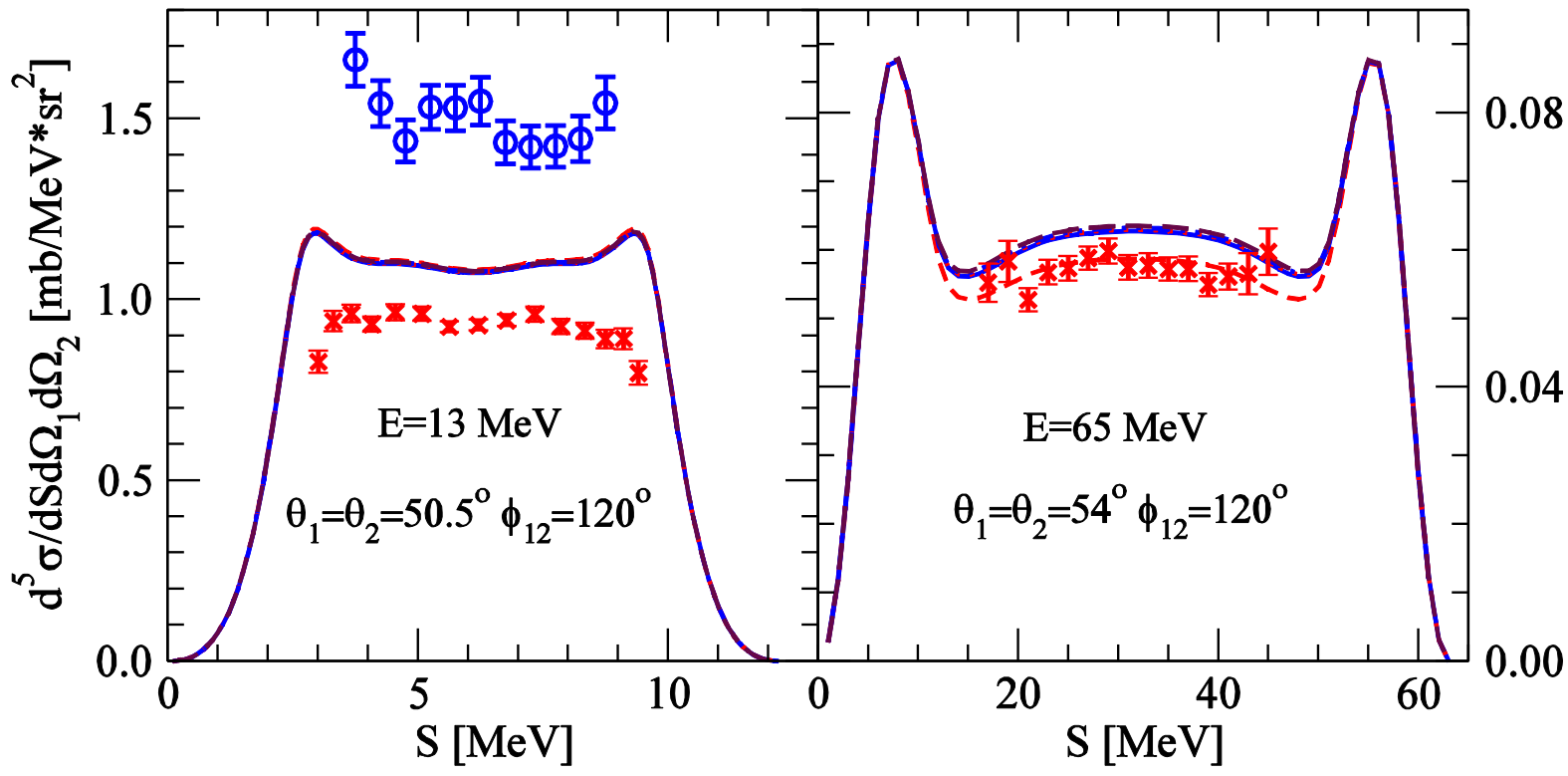

FIG. 6: (Color online) The nd breakup five-fold differential cross section in the SST complete geometry at the incoming neutron laboratory energies $E = 13$ MeV and $E = 65$ MeV, shown as a function of arc-length of the S-curve. The dashed (red) lines are predictions of the N^{4}LO SCS NN potential with the regulator $R = 0.9$ fm. Combining that NN potential with the N^{2}LO 3NF with four different strengths (c_D, c_E) of the contact terms from the corelation line of Fig.1 leads to results shown by different lines: solid (blue) $(4.0, -0.270)$, dotted (red) $(6.0, -1.094)$, double-dotted-dashed (blue) $(8.0, -2.032)$, and dashed (maroon) $(10.0, -3.108)$. At $E = 13$ MeV the (blue) circles are nd data from Ref. [42] and the (red) x-ces are pd data from Ref. [43]. At $E = 65$ MeV the (red) x-ces are pd data from Ref. [28].

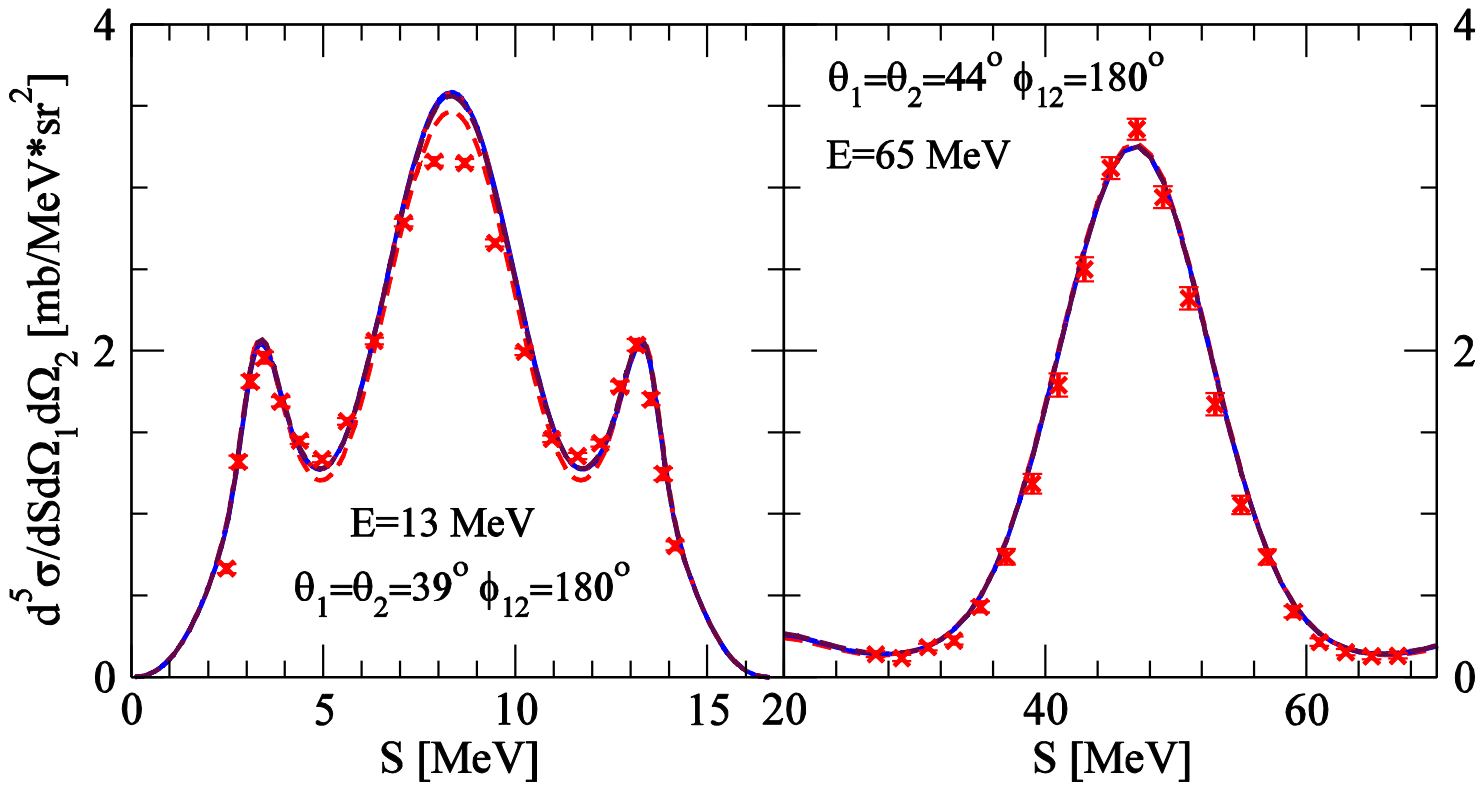

FIG. 7: (Color online) The nd breakup five-fold differential cross section in the QFS complete geometry at the incoming neutron laboratory energies $E = 13$ MeV and $E = 65$ MeV, shown as a function of arc-length of the S-curve. For description of lines see Fig. 6. The (red) x-ces are pd data from Ref. [43] at $E = 13$ MeV and from Ref. [44] at $E = 65$ MeV.

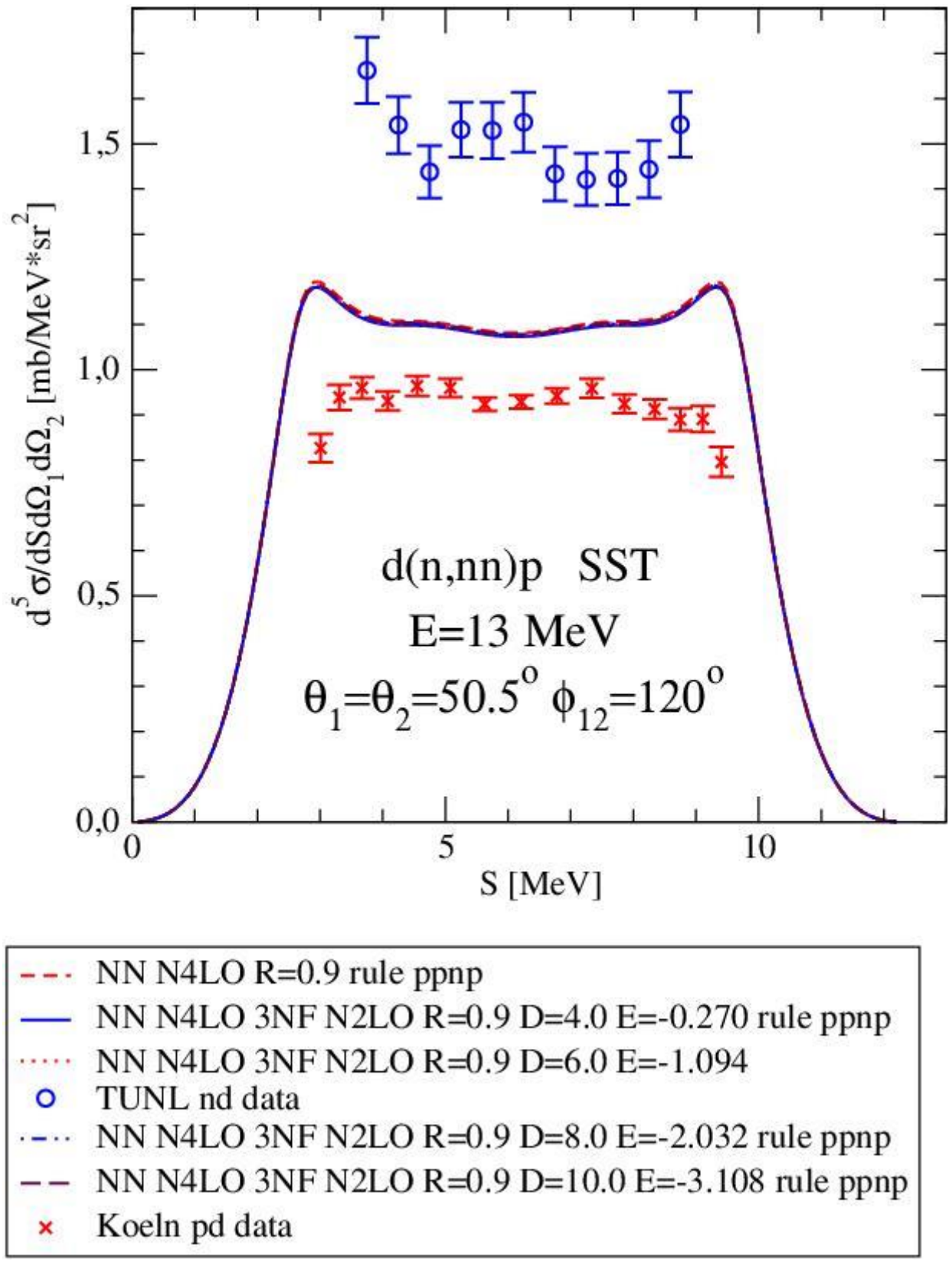

- practically no 3NF effects (at N2LO) for that configuration

Calculation of Proton-Deuteron Breakup Reactions including the Coulomb Interaction between the Two Protons

A. Deltuva,[1,*] A. C. Fonseca,[1] and P. U. Sauer[2]

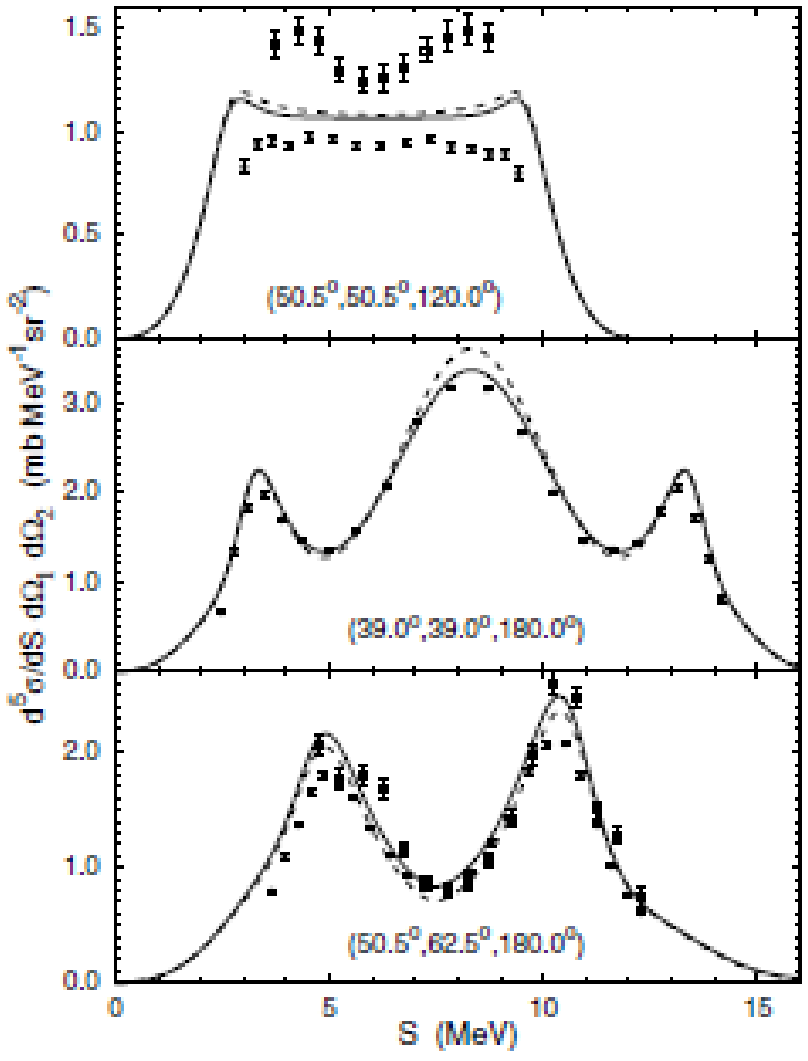

FIG. 2. Differential cross section for *pd* breakup at 13 MeV proton lab energy for space star, quasi-free scattering, and collinear configurations (from top to bottom). Results for CD Bonn $+\Delta$ potential including the Coulomb interaction (solid curves) are compared to results without Coulomb (dashed curves). The experimental *pd* data (circles) are from Ref. [18] and *nd* data (squares) are from Ref. [19].

- practically no pp Coulomb force effects for low energy space star configuration !

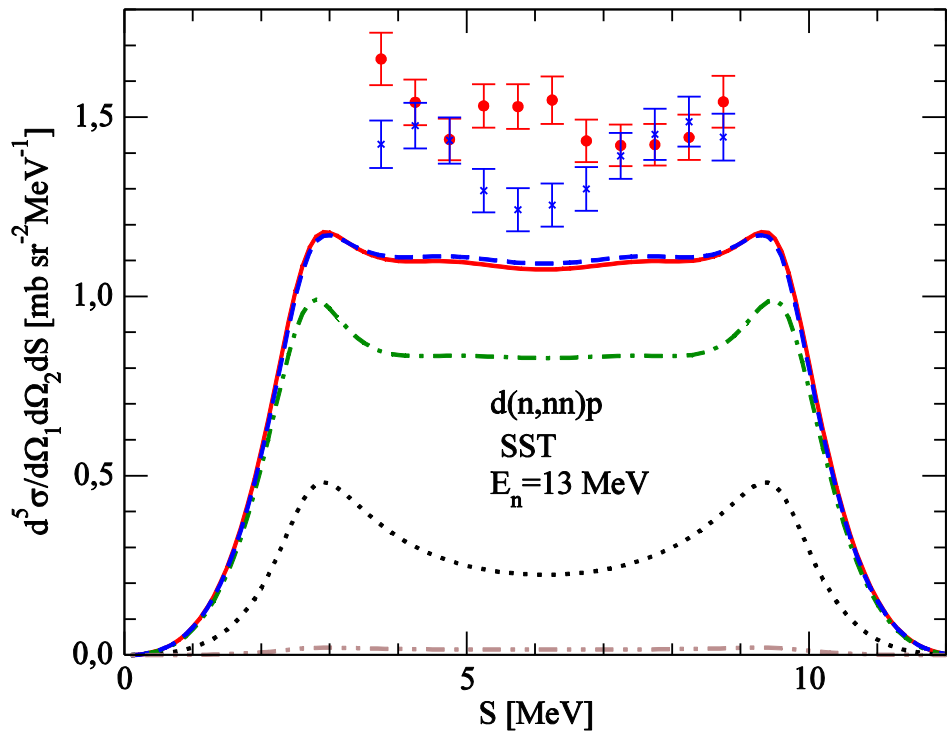

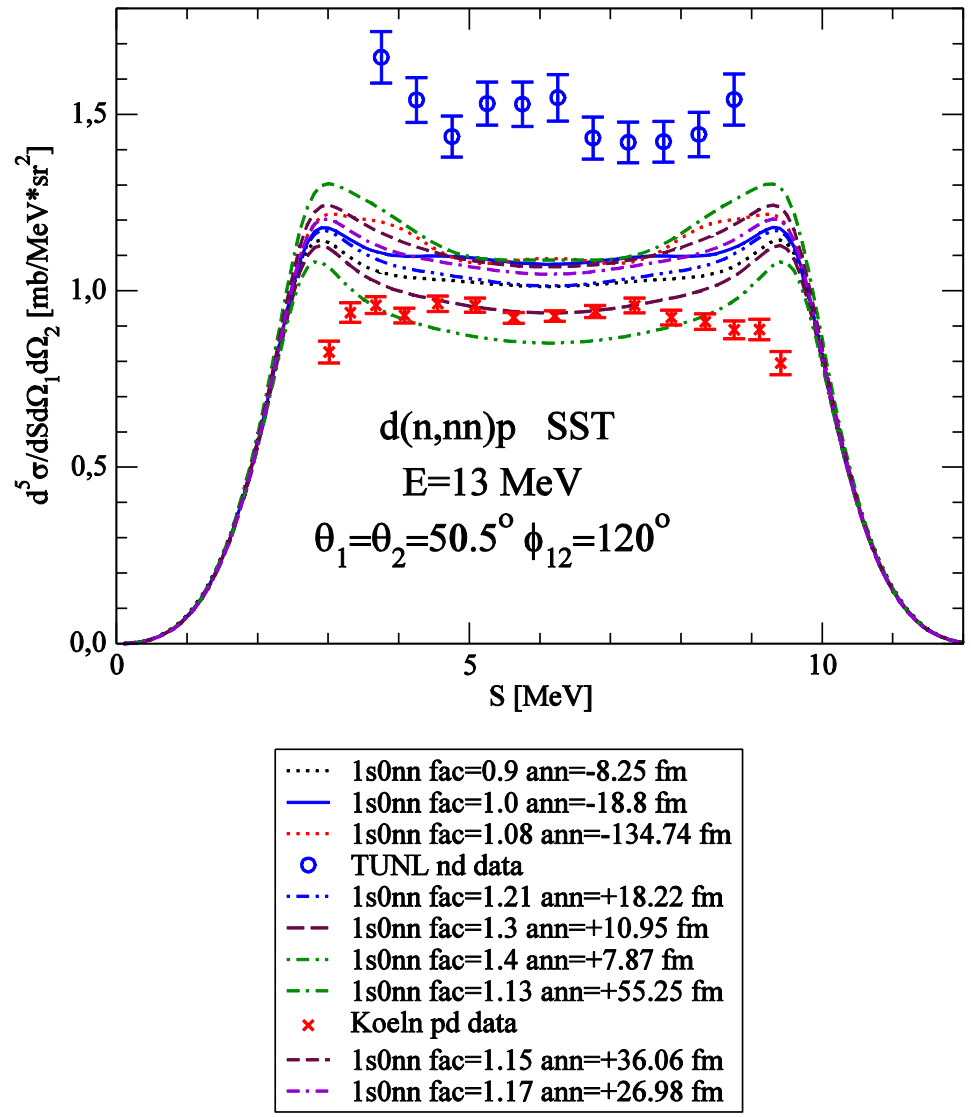

- only $^1S_0$ and $^3S_1$ contribute at this energy
- is something wrong with $^1S_0$ (nn or pp) at low energies ?

- making $^1S_0$ nn stronger (positive scattering length - bound $^1S_0$ nn state) could explain pd data (but not nd data !)

Various topologies contributing to the 3NF up to and including N^4LO

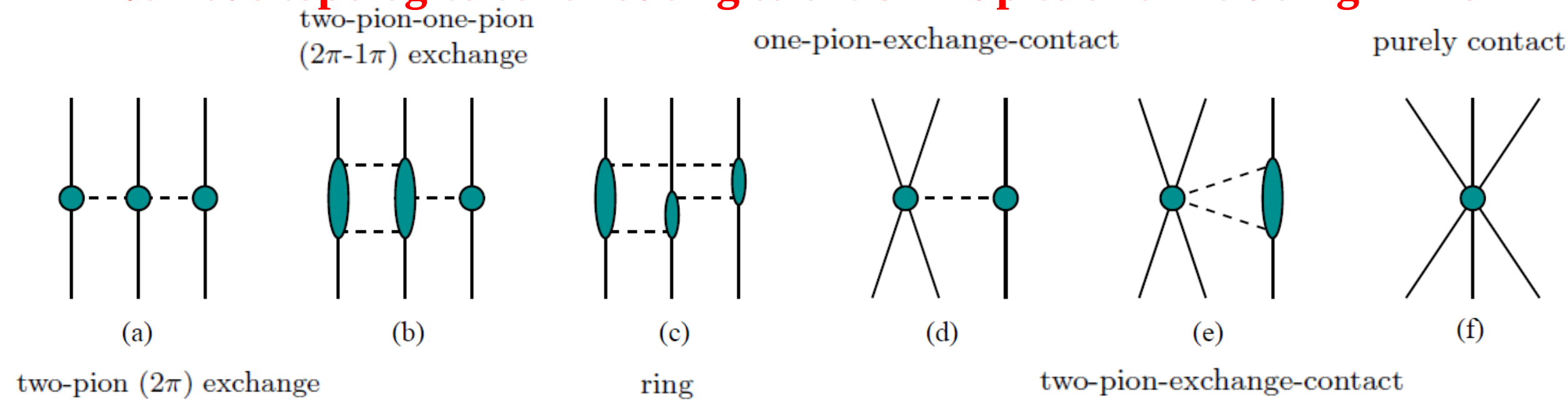

- N^2LO: (a) + (d) + (f) (E.Epelbaum et al., PR C66, 064001 (2002))

- N^3LO: (a) + (b) + (c) + (d) + (e) + (f) + rel
  V.Bernard et al., PR C77, 064004 (2008) - long range contributions (a), (b), (c)
  V.Bernard et al., PR C84, 054001 (2011) - short range terms (e)
  and leading relativistic corrections

N^3LO contributions do not involve any unknown low energy constants !

The full N^3LO 3NF depends on two parameters c_D and c_E coming with (d) and (f) terms, respectively. They are adjusted to two chosen 3N observables.

- N^4LO (longest range contributions): (a) + (b) + (c) + (d) + (e) + (f) (H.Krebs et al., arXiv:1203.0067)

A_y puzzle: N^3LO 3NF with short-ranged 2π-contact term

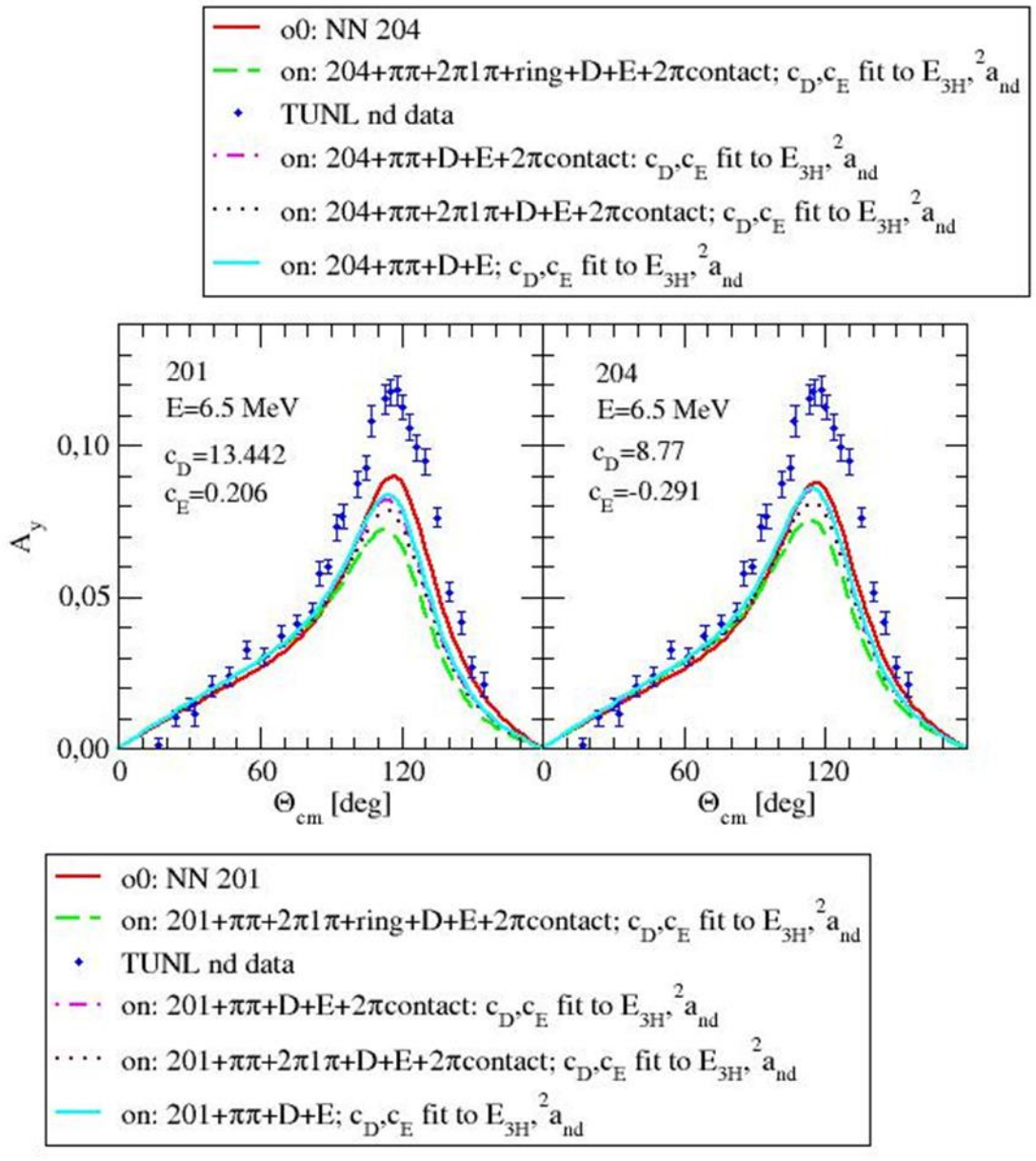

Breakup symmetric-space-star (SST) configuration:

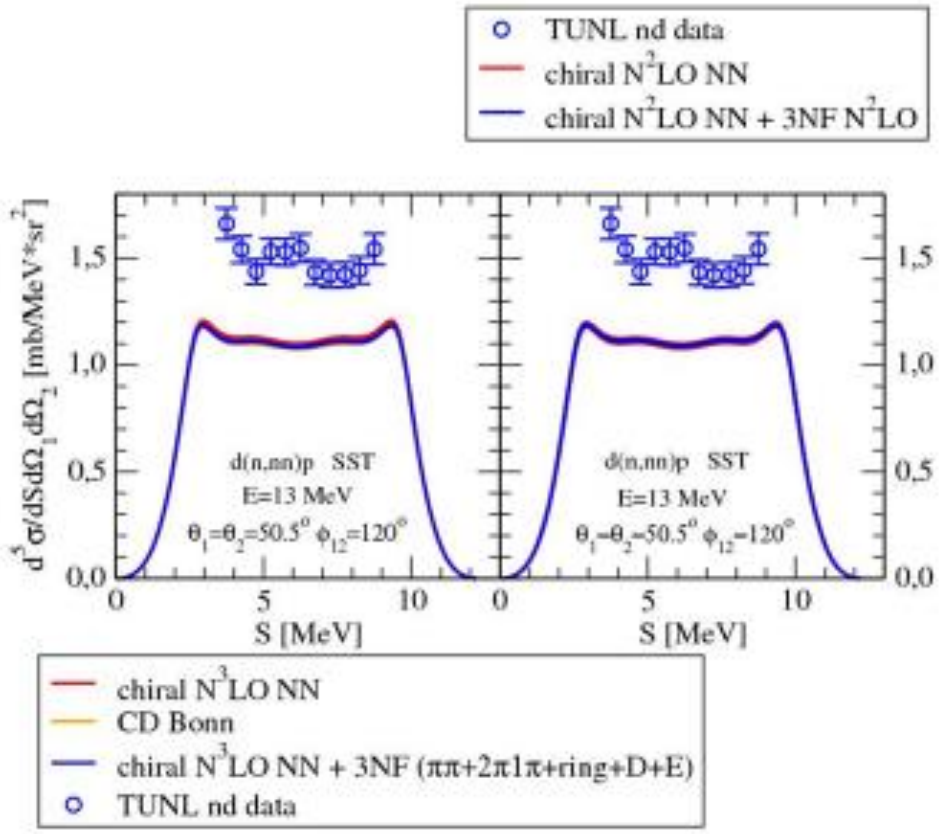

Breakup quasi-free-scattering (QFS) configuration:

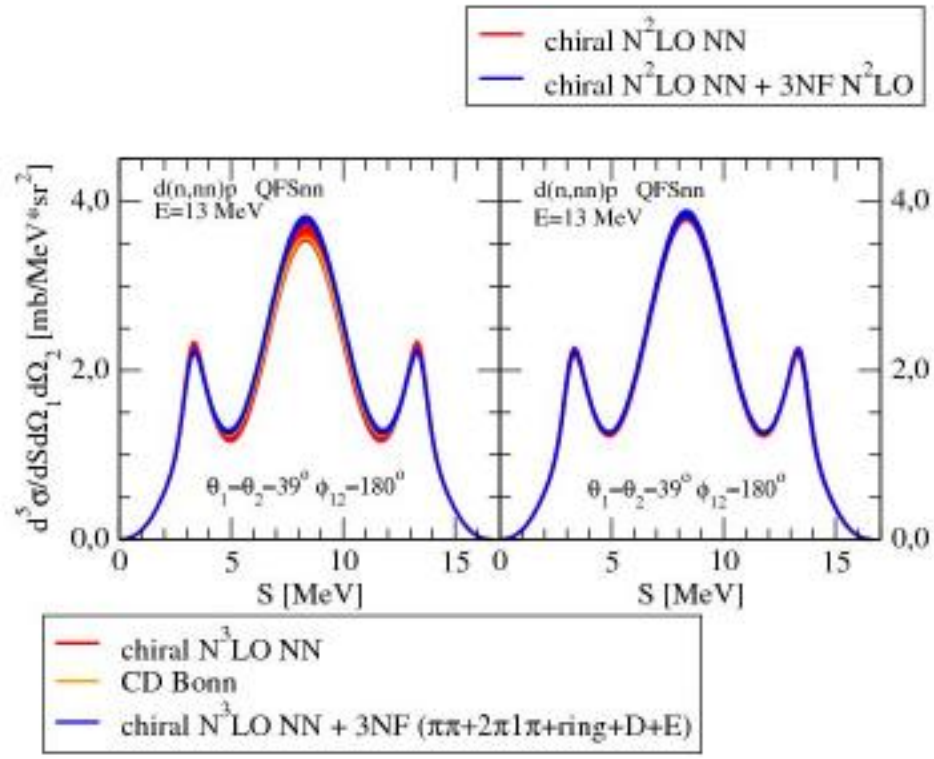

Conclusions:

- ❑ at low energies effects of N^3LO 3NF's are rather small
- ❑ they do not decrease the discrepancy between data and theory in the maximum of A_y

PHYSICAL REVIEW C **84**, 014001 (2011)

Subleading contributions to the three-nucleon contact interaction

L. Girlanda,[1] A. Kievsky,[2] and M. Viviani[2]
[1]*Dipartimento di Fisica, Università del Salento, and INFN Sezione di Lecce, Via Arnesano, I-73100 Lecce, Italy*
[2]*INFN, Sezione di Pisa, Largo Bruno Pontecorvo 3, I-56127 Pisa, Italy*
(Received 23 February 2011; published 8 July 2011)

We obtain a minimal form of the two-derivative three-nucleon contact Lagrangian, by imposing all constraints deriving from discrete symmetries, Fierz identities, and Poincaré covariance. The resulting interaction, depending on 10 unknown low-energy constants, leads to a three-nucleon potential which we give in a local form in configuration space. We also consider the leading (no-derivative) four-nucleon interaction and show that there exists only one independent operator.

V. THE SUBLEADING THREE-NUCLEON CONTACT POTENTIAL

The $3N$ potential is obtained by taking the matrix element of the interaction between $3N$ states. By denoting $\mathbf{k}_i = \mathbf{p}_i - \mathbf{p}'_i$ and $\mathbf{Q}_i = \mathbf{p}_i + \mathbf{p}'_i$, $\mathbf{p}_i$ and $\mathbf{p}'_i$ being the initial and final momenta of nucleon i, the potential in momentum space is found to be

$$\begin{aligned} V = \sum_{i\neq j\neq k} \Big[& -E_1 \mathbf{k}_i^2 - E_2 \mathbf{k}_i^2 \boldsymbol{\tau}_i \cdot \boldsymbol{\tau}_j - E_3 \mathbf{k}_i^2 \boldsymbol{\sigma}_i \cdot \boldsymbol{\sigma}_j \\ & - E_4 \mathbf{k}_i^2 \boldsymbol{\sigma}_i \cdot \boldsymbol{\sigma}_j \boldsymbol{\tau}_i \cdot \boldsymbol{\tau}_j - E_5 \left(3\mathbf{k}_i \cdot \boldsymbol{\sigma}_i \mathbf{k}_i \cdot \boldsymbol{\sigma}_j - \mathbf{k}_i^2\right) \\ & - E_6 \left(3\mathbf{k}_i \cdot \boldsymbol{\sigma}_i \mathbf{k}_i \cdot \boldsymbol{\sigma}_j - \mathbf{k}_i^2\right) \boldsymbol{\tau}_i \cdot \boldsymbol{\tau}_j \\ & + \frac{i}{2} E_7 \mathbf{k}_i \left(\mathbf{Q}_i - \mathbf{Q}_j\right) \cdot (\boldsymbol{\sigma}_i + \boldsymbol{\sigma}_j) \\ & + \frac{i}{2} E_8 \mathbf{k}_i \times (\mathbf{Q}_i - \mathbf{Q}_j) \cdot (\boldsymbol{\sigma}_i + \boldsymbol{\sigma}_j) \boldsymbol{\tau}_j \cdot \boldsymbol{\tau}_k \\ & - E_9 \mathbf{k}_i \cdot \boldsymbol{\sigma}_i \mathbf{k}_j \cdot \boldsymbol{\sigma}_j - E_{10} \mathbf{k}_i \cdot \boldsymbol{\sigma}_i \mathbf{k}_j \cdot \boldsymbol{\sigma}_j \boldsymbol{\tau}_i \cdot \boldsymbol{\tau}_j \Big], \end{aligned} \quad (15)$$

E.Epelbaum, P.Reinert, HW:

Exploration of the effects of the N4LO contact 3NF of the c_{E1}, c_{E7} type

Calculations are performed using the 3NF of the kind:

$$V_{3N} = V_{3N}^{N2LO} + E_1 \sum_{i\neq j\neq k} q_i^2 + iE_7 \sum_{i\neq j\neq k} \vec{q}_i \times (\vec{k}_i - \vec{k}_j) \cdot (\vec{\sigma}_i + \vec{\sigma}_j)$$

where $\vec{k}_i \equiv \frac{1}{2}(\vec{p}_i + \vec{p}_j)$. Further, dimensionless LECs are defined as $E_i = \frac{c_{E_i}}{F_\pi^4 \Lambda^3}$ with $\Lambda = 700$ MeV.

All calculations are performed using the SMS N^4LO^+ interaction with $\Lambda = 450$ MeV

Otherwise the same procedure is used as for the N^2LO 2NF + 3NF calculations:

- for fixed values of c_{E1} and c_{E7}, the LECs c_D and c_E are determined from the ^3H BE and the cross section minimum at $E_N = 70$ MeV. The c_D-c_E correlation fits were performed by Patrick. Nd scattering calculations done in the usual way with $j_{max} = 5$ and the 3NF is included up to J = 7/2.

- Altogether, 9 calculations have been performed: $c_{E1} = c_{E7} = 0$ (standard N^2LO) and $c_{E1} = \{-4, -2, 2, 4\}$, $c_{E7} = 0$ as well as $c_{E1} = 0$, $c_{E7} = \{-4, -2, 2, 4\}$.

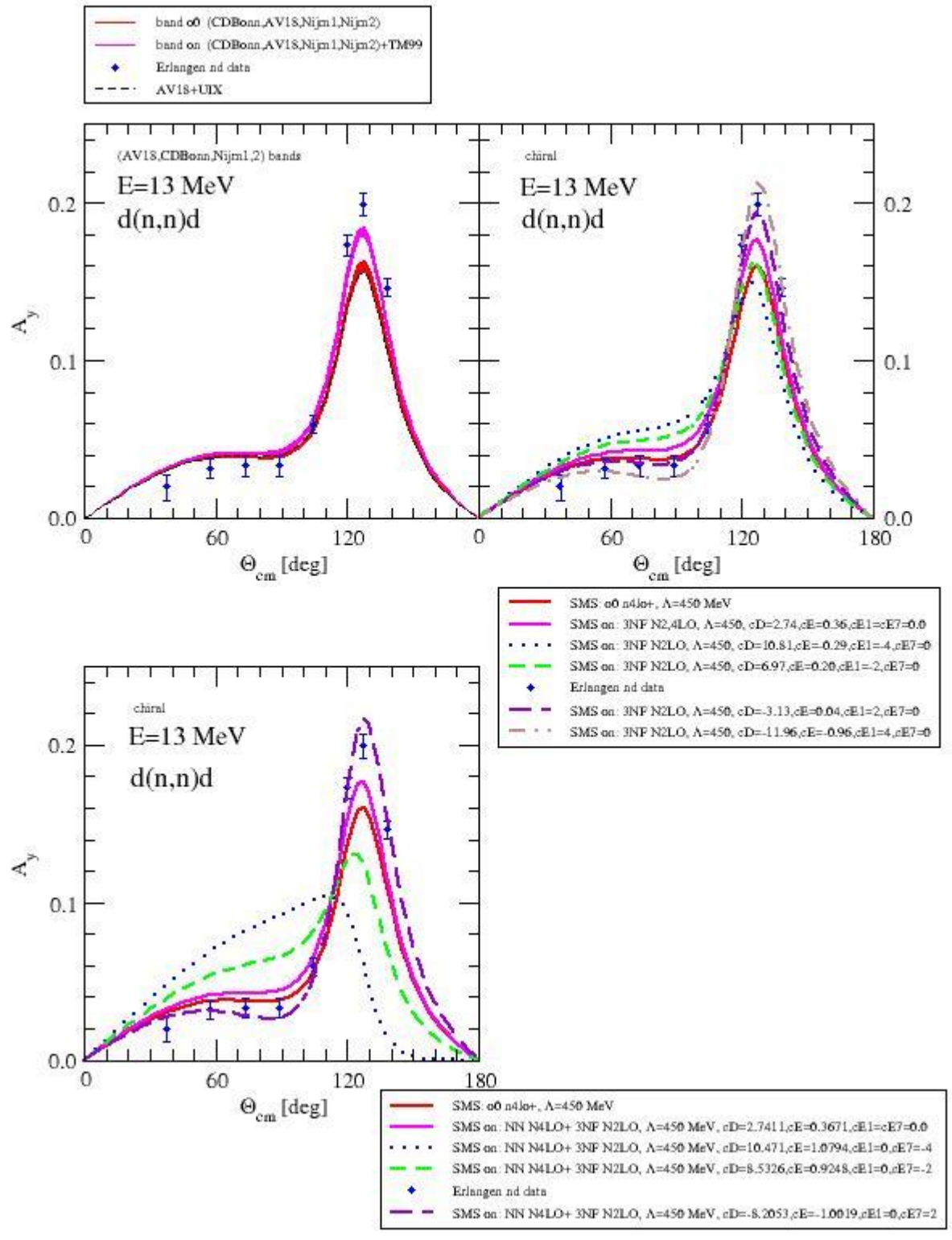
band o0 (CDBonn,AV18,Nijm1,Nijm2)
band on (CDBonn,AV18,Nijm1,Nijm2)+TM99
Erlangen nd data
AV18+UIX
(AV18,CDBonn,Nijm1,2) bands
E=13 MeV
d(n,n)d
chiral
E=13 MeV
d(n,n)d
A_y
Θ_{cm} [deg]
SMS: o0 n4lo+, Λ=450 MeV
SMS on: 3NF N2,4LO, Λ=450, cD=2.74,cE=0.36,cE1=cE7=0.0
SMS on: 3NF N2LO, Λ=450, cD=10.81,cE=-0.29,cE1=-4,cE7=0
SMS on: 3NF N2LO, Λ=450, cD=6.97,cE=0.20,cE1=-2,cE7=0
Erlangen nd data
SMS on: 3NF N2LO, Λ=450, cD=-3.13,cE=0.04,cE1=2,cE7=0
SMS on: 3NF N2LO, Λ=450, cD=-11.96,cE=-0.96,cE1=4,cE7=0
chiral
E=13 MeV
d(n,n)d
A_y
Θ_{cm} [deg]
SMS: o0 n4lo+, Λ=450 MeV
SMS on: NN N4LO+ 3NF N2LO, Λ=450 MeV, cD=2.7411,cE=0.3671,cE1=cE7=0.0
SMS on: NN N4LO+ 3NF N2LO, Λ=450 MeV, cD=10.471,cE=1.0794,cE1=0,cE7=-4
SMS on: NN N4LO+ 3NF N2LO, Λ=450 MeV, cD=8.5326,cE=0.9248,cE1=0,cE7=-2
Erlangen nd data
SMS on: NN N4LO+ 3NF N2LO, Λ=450 MeV, cD=-8.2053,cE=-1.0019,cE1=0,cE7=2

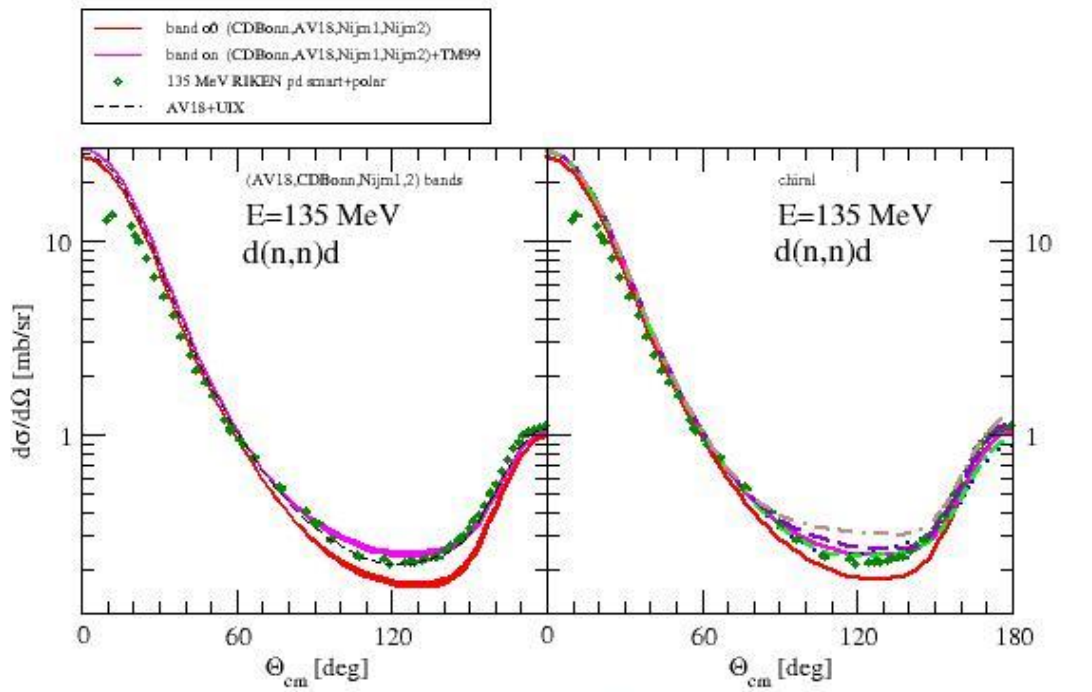
band σ0 (CDBonn,AV18,Nijm1,Nijm2)
band σn (CDBonn,AV18,Nijm1,Nijm2)+TM99
135 MeV RIKEN pd smart+polar
AV18+UIX
(AV18,CDBonn,Nijm1,2) bands
E=135 MeV
d(n,n)d
chiral
E=135 MeV
d(n,n)d
dσ/dΩ [mb/sr]
Θcm [deg]
SMS: σ0 n4lo+, Λ=450 MeV
SMS σn: 3NF N2,4LO, Λ=450, cD=2.74,cE=0.36,cE1=cE7=0.0
SMS σn: 3NF N2LO, Λ=450, cD=10.81,cE=-0.29,cE1=-4,cE7=0
SMS σn: 3NF N2LO, Λ=450, cD=6.97,cE=0.20,cE1=-2,cE7=0
135 MeV pd RIKEN smart+polar
SMS σn: 3NF N2LO, Λ=450, cD=-3.13,cE=0.04,cE1=2,cE7=0
SMS σn: 3NF N2LO, Λ=450, cD=-11.96,cE=-0.96,cE1=4,cE7=0
chiral
E=135 MeV
d(n,n)d
SMS: σ0 n4lo+, Λ=450 MeV
SMS σn: NN N4LO+ 3NF N2LO, Λ=450 MeV, cD=2.7411,cE=0.3671,cE1=cE7=0.0
SMS σn: NN N4LO+ 3NF N2LO, Λ=450 MeV, cD=10.471,cE=1.0794,cE1=0,cE7=-4
SMS σn: NN N4LO+ 3NF N2LO, Λ=450 MeV, cD=8.5326,cE=0.9248,cE1=0,cE7=-2
135 MeV RIKEN pd smart+polar
SMS σn: NN N4LO+ 3NF N2LO, Λ=450 MeV, cD=-8.2053,cE=-1.0019,cE1=0,cE7=2

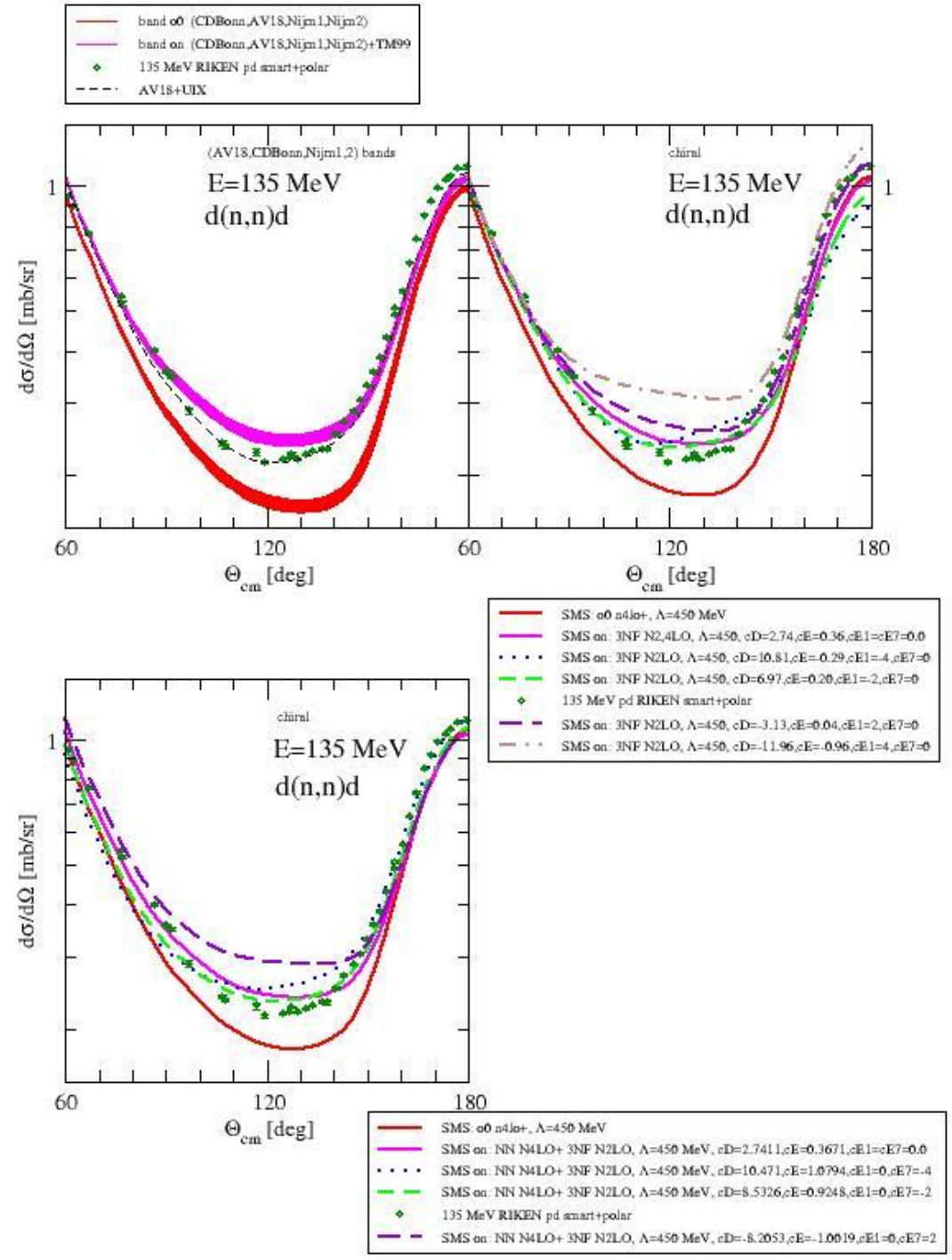
band σ0 (CDBonn,AV18,Nijm1,Nijm2)
band σn (CDBonn,AV18,Nijm1,Nijm2)+TM99
135 MeV RIKEN pd smart+polar
AV18+UIX
(AV18,CDBonn,Nijm1,2) bands
E=135 MeV
d(n,n)d
chiral
E=135 MeV
d(n,n)d
dσ/dΩ [mb/sr]
Θcm [deg]
SMS: σ0 n4lo+, Λ=450 MeV
SMS σn: 3NF N2,4LO, Λ=450, cD=2.74,cE=0.36,cE1=cE7=0.0
SMS σn: 3NF N2LO, Λ=450, cD=10.81,cE=-0.29,cE1=-4,cE7=0
SMS σn: 3NF N2LO, Λ=450, cD=6.97,cE=0.20,cE1=-2,cE7=0
135 MeV pd RIKEN smart+polar
SMS σn: 3NF N2LO, Λ=450, cD=-3.13,cE=0.04,cE1=2,cE7=0
SMS σn: 3NF N2LO, Λ=450, cD=-11.96,cE=-0.96,cE1=4,cE7=0
chiral
E=135 MeV
d(n,n)d
SMS: σ0 n4lo+, Λ=450 MeV
SMS σn: NN N4LO+ 3NF N2LO, Λ=450 MeV, cD=2.7411,cE=0.3671,cE1=cE7=0.0
SMS σn: NN N4LO+ 3NF N2LO, Λ=450 MeV, cD=10.471,cE=1.0794,cE1=0,cE7=-4
SMS σn: NN N4LO+ 3NF N2LO, Λ=450 MeV, cD=8.5326,cE=0.9248,cE1=0,cE7=-2
135 MeV RIKEN pd smart+polar
SMS σn: NN N4LO+ 3NF N2LO, Λ=450 MeV, cD=-8.2053,cE=-1.0019,cE1=0,cE7=2

band o0 (CDBonn,AV18,Nijm1,Nijm2)
band on (CDBonn,AV18,Nijm1,Nijm2)+TM99
2H(n,n) cross-section data at 190.00 MeV - (measured at LANL/WNR)
AV18+UIX
pd KVI 190 MeV

(AV18,CDBonn,Nijm1,2) bands
E=190 MeV
d(n,n)d

chiral
E=190 MeV
d(n,n)d

$d\sigma/d\Omega$ [mb/sr]

Θ_{cm} [deg]

band o0 (CDBonn,AV18,Nijm1,Nijm2)
band on (CDBonn,AV18,Nijm1,Nijm2)+TM99
2H(n,n) cross-section data at 190.00 MeV - (measured at LANL/WNR)
AV18+UIX
pd KVI 190 MeV

(AV18,CDBonn,Nijm1,2) bands
E=190 MeV
d(n,n)d

chiral
E=190 MeV
d(n,n)d

$d\sigma/d\Omega$ [mb/sr]

Θ_{cm} [deg]

SMS: o0 n4lo+, Λ=450 MeV
SMS on: 3NF N2,4LO, Λ=450, cD=2.74,cE=0.36,cE1=cE7=0.0
SMS on: 3NF N2LO, Λ=450, cD=10.81,cE=-0.29,cE1=-4,cE7=0
SMS on: 3NF N2LO, Λ=450, cD=6.97,cE=0.20,cE1=-2,cE7=0
2H(n,n) cross-section data at 190.00 MeV - (measured at LANL/WNR)
SMS on: 3NF N2LO, Λ=450, cD=-3.13,cE=-0.04,cE1=2,cE7=0
SMS on: 3NF N2LO, Λ=450, cD=-11.96,cE=-0.96,cE1=4,cE7=0
pd KVI 190 MeV

chiral
E=190 MeV
d(n,n)d

$d\sigma/d\Omega$ [mb/sr]

Θ_{cm} [deg]

SMS: o0 n4lo+, Λ=450 MeV
SMS on: 3NF N2,4LO, Λ=450, cD=2.74,cE=0.36,cE1=cE7=0.0
SMS on: 3NF N2LO, Λ=450, cD=10.81,cE=-0.29,cE1=-4,cE7=0
SMS on: 3NF N2LO, Λ=450, cD=6.97,cE=0.20,cE1=-2,cE7=0
2H(n,n) cross-section data at 190.00 MeV - (measured at LANL/WNR)
SMS on: 3NF N2LO, Λ=450, cD=-3.13,cE=-0.04,cE1=2,cE7=0
SMS on: 3NF N2LO, Λ=450, cD=-11.96,cE=-0.96,cE1=4,cE7=0
pd KVI 190 MeV

SMS: o0 n4lo+, Λ=450 MeV
SMS on: NN N4LO+ 3NF N2LO, Λ=450 MeV, cD=2.7411,cE=0.3671,cE1=cE7=0.0
SMS on: NN N4LO+ 3NF N2LO, Λ=450 MeV, cD=10.471,cE=1.0794,cE1=0,cE7=-4
SMS on: NN N4LO+ 3NF N2LO, Λ=450 MeV, cD=8.5326,cE=0.9248,cE1=0,cE7=-2
2H(n,n) cross-section data at 190.00 MeV - (measured at LANL/WNR)
SMS on: NN N4LO+ 3NF N2LO, Λ=450 MeV, cD=-8.2053,cE=-1.0019,cE1=0,cE7=2
pd KVI 190 MeV

SMS: o0 n4lo+, Λ=450 MeV
SMS on: NN N4LO+ 3NF N2LO, Λ=450 MeV, cD=2.7411,cE=0.3671,cE1=cE7=0.0
SMS on: NN N4LO+ 3NF N2LO, Λ=450 MeV, cD=10.471,cE=1.0794,cE1=0,cE7=-4
SMS on: NN N4LO+ 3NF N2LO, Λ=450 MeV, cD=8.5326,cE=0.9248,cE1=0,cE7=-2
2H(n,n) cross-section data at 190.00 MeV - (measured at LANL/WNR)
SMS on: NN N4LO+ 3NF N2LO, Λ=450 MeV, cD=-8.2053,cE=-1.0019,cE1=0,cE7=2
pd KVI 190 MeV

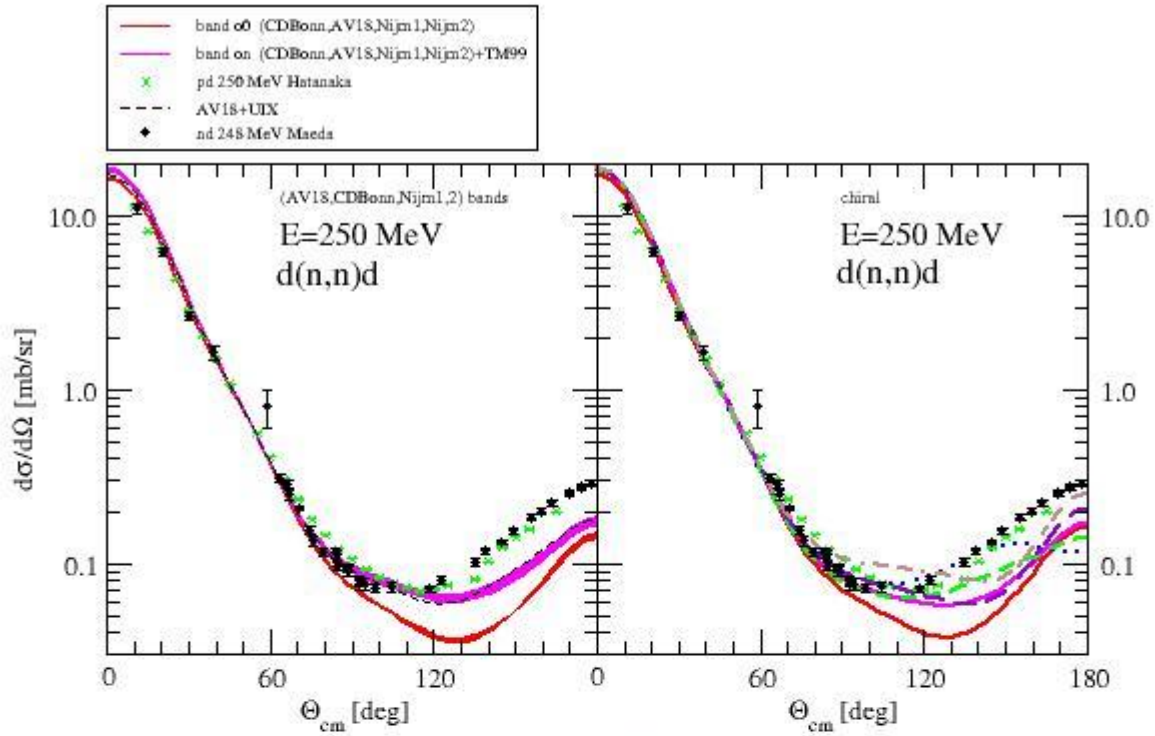
band o0 (CDBonn,AV18,Nijm1,Nijm2)
band on (CDBonn,AV18,Nijm1,Nijm2)+TM99
pd 250 MeV Hatanaka
AV18+UIX
nd 248 MeV Maeda
(AV18,CDBonn,Nijm1,2) bands
E=250 MeV
d(n,n)d
chiral
E=250 MeV
d(n,n)d
dσ/dΩ [mb/sr]
Θcm [deg]

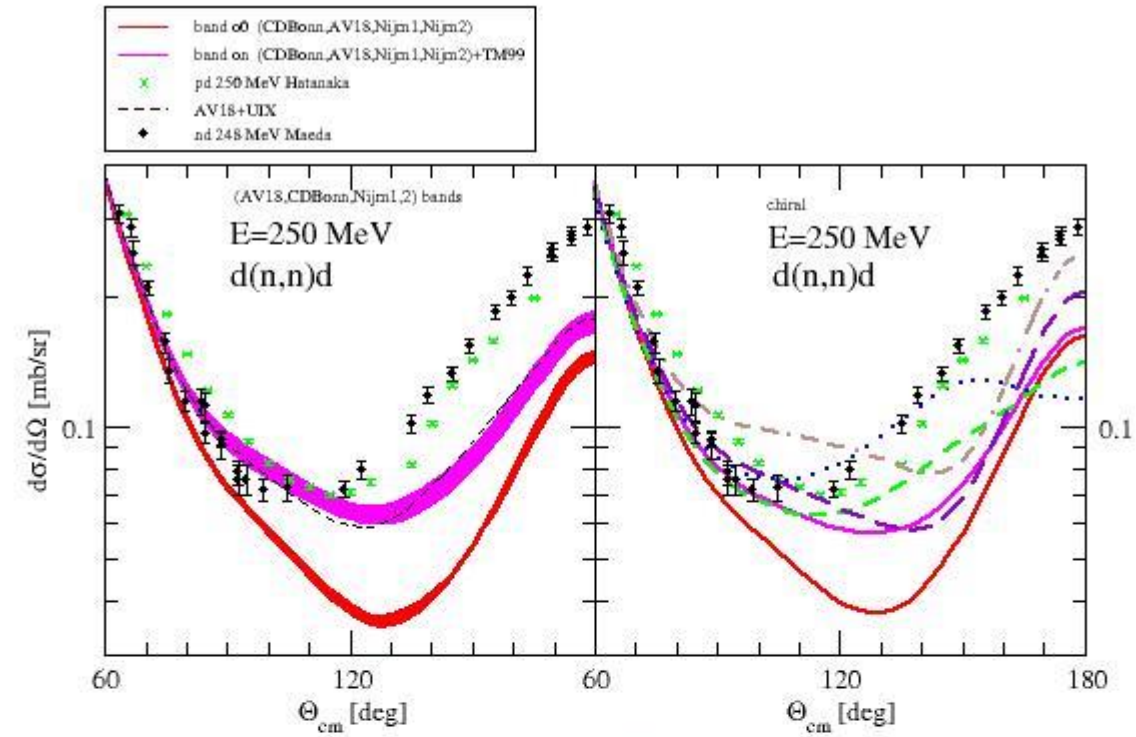
band o0 (CDBonn,AV18,Nijm1,Nijm2)
band on (CDBonn,AV18,Nijm1,Nijm2)+TM99
pd 250 MeV Hatanaka
AV18+UIX
nd 248 MeV Maeda
(AV18,CDBonn,Nijm1,2) bands
E=250 MeV
d(n,n)d
chiral
E=250 MeV
d(n,n)d
dσ/dΩ [mb/sr]
Θcm [deg]

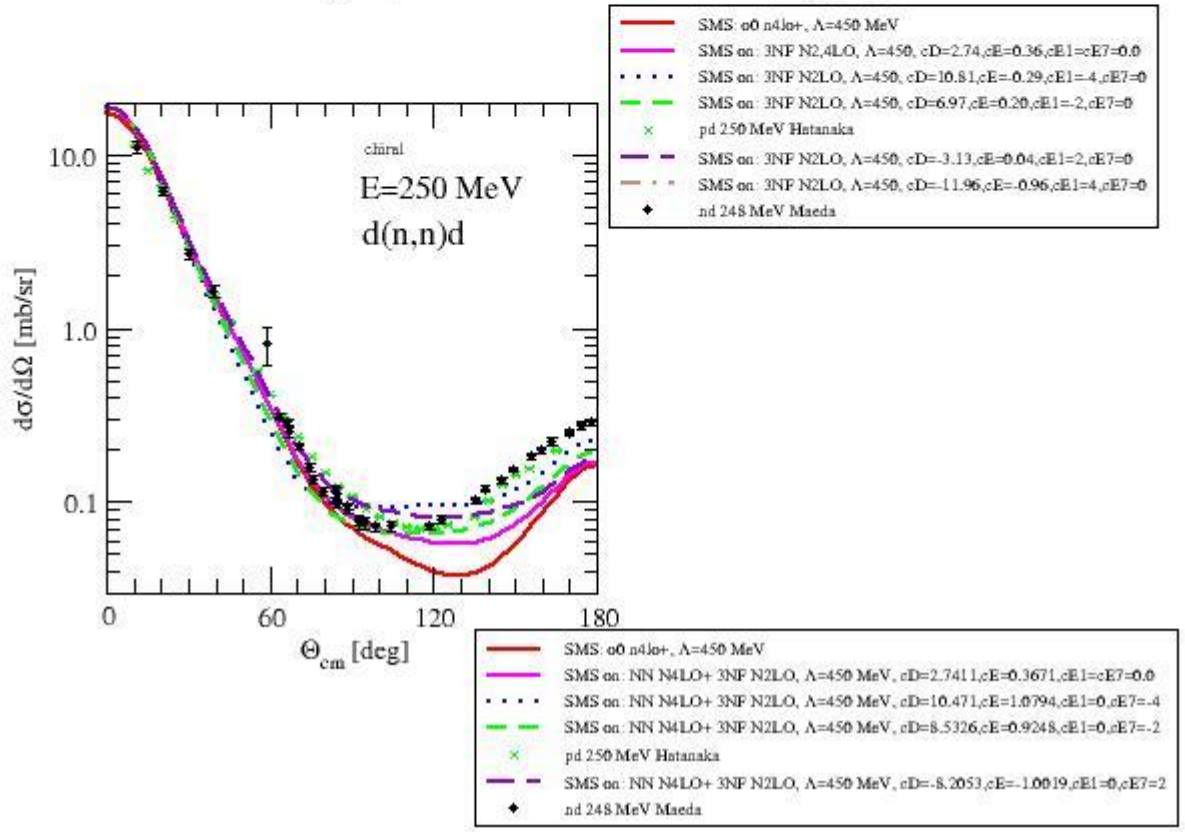
SMS: o0 n4lo+, Λ=450 MeV
SMS on: 3NF N2,4LO, Λ=450, cD=2.74,cE=0.36,cE1=cE7=0.0
SMS on: 3NF N2LO, Λ=450, cD=10.81,cE=-0.29,cE1=-4,cE7=0
SMS on: 3NF N2LO, Λ=450, cD=6.97,cE=0.20,cE1=-2,cE7=0
pd 250 MeV Hatanaka
SMS on: 3NF N2LO, Λ=450, cD=-3.13,cE=0.04,cE1=2,cE7=0
SMS on: 3NF N2LO, Λ=450, cD=-11.96,cE=-0.96,cE1=4,cE7=0
nd 248 MeV Maeda
chiral
E=250 MeV
d(n,n)d
dσ/dΩ [mb/sr]
Θcm [deg]
SMS: o0 n4lo+, Λ=450 MeV
SMS on: NN N4LO+ 3NF N2LO, Λ=450 MeV, cD=2.7411,cE=0.3671,cE1=cE7=0.0
SMS on: NN N4LO+ 3NF N2LO, Λ=450 MeV, cD=10.471,cE=1.0794,cE1=0,cE7=-4
SMS on: NN N4LO+ 3NF N2LO, Λ=450 MeV, cD=8.5326,cE=0.9248,cE1=0,cE7=-2
pd 250 MeV Hatanaka
SMS on: NN N4LO+ 3NF N2LO, Λ=450 MeV, cD=-8.2053,cE=-1.0019,cE1=0,cE7=2
nd 248 MeV Maeda

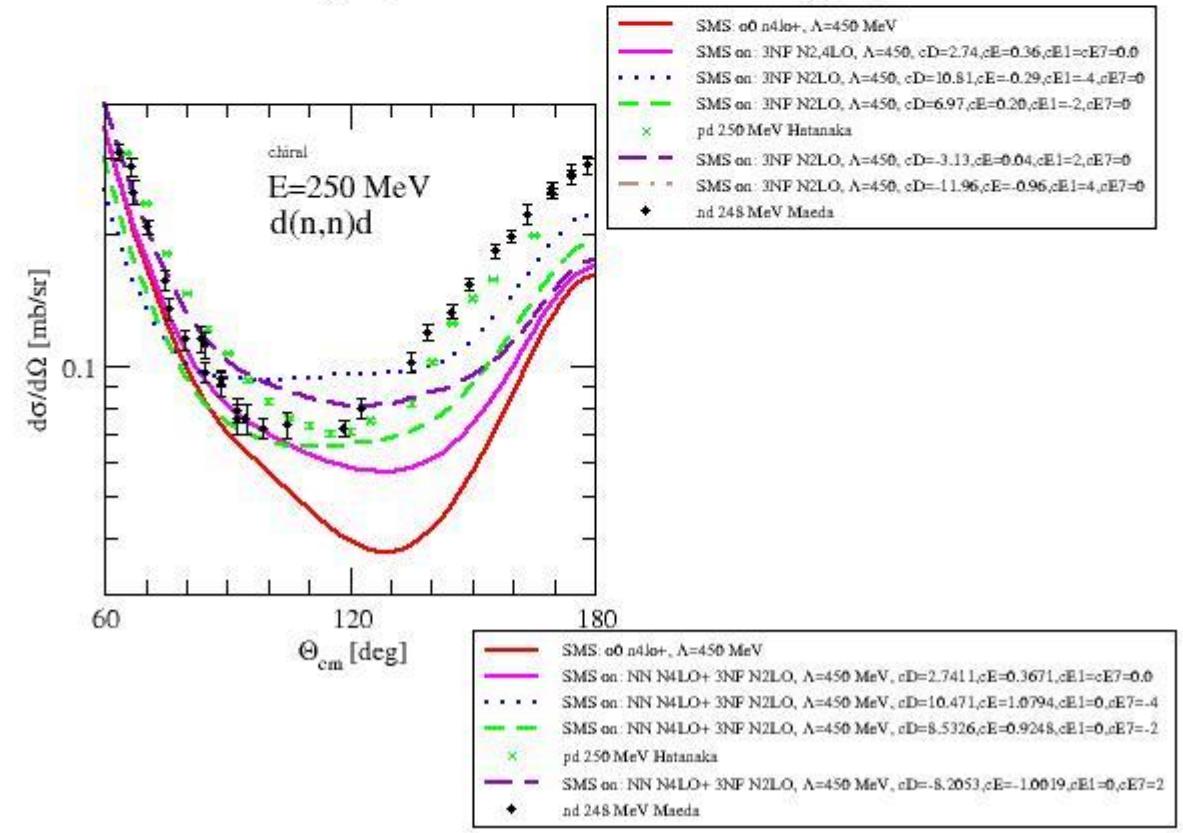
SMS: o0 n4lo+, Λ=450 MeV
SMS on: 3NF N2,4LO, Λ=450, cD=2.74,cE=0.36,cE1=cE7=0.0
SMS on: 3NF N2LO, Λ=450, cD=10.81,cE=-0.29,cE1=-4,cE7=0
SMS on: 3NF N2LO, Λ=450, cD=6.97,cE=0.20,cE1=-2,cE7=0
pd 250 MeV Hatanaka
SMS on: 3NF N2LO, Λ=450, cD=-3.13,cE=0.04,cE1=2,cE7=0
SMS on: 3NF N2LO, Λ=450, cD=-11.96,cE=-0.96,cE1=4,cE7=0
nd 248 MeV Maeda
chiral
E=250 MeV
d(n,n)d
dσ/dΩ [mb/sr]
Θcm [deg]
SMS: o0 n4lo+, Λ=450 MeV
SMS on: NN N4LO+ 3NF N2LO, Λ=450 MeV, cD=2.7411,cE=0.3671,cE1=cE7=0.0
SMS on: NN N4LO+ 3NF N2LO, Λ=450 MeV, cD=10.471,cE=1.0794,cE1=0,cE7=-4
SMS on: NN N4LO+ 3NF N2LO, Λ=450 MeV, cD=8.5326,cE=0.9248,cE1=0,cE7=-2
pd 250 MeV Hatanaka
SMS on: NN N4LO+ 3NF N2LO, Λ=450 MeV, cD=-8.2053,cE=-1.0019,cE1=0,cE7=2
nd 248 MeV Maeda

band o0 (CDBonn,AV18,Nijm1,Nijm2)
band on (CDBonn,AV18,Nijm1,Nijm2)+TM99
pd 250 MeV Hatanaka
AV18+UIX

(AV18,CDBonn,Nijm1,2) bands
E=250 MeV
d(n,n)d

chiral
E=250 MeV
d(n,n)d

A_y

iT_{11}

Θ_{cm} [deg]

SMS: o0 n4lo+, Λ=450 MeV
SMS on: 3NF N2,4LO, Λ=450, cD=2.74,cE=0.36,cE1=cE7=0.0
SMS on: 3NF N2LO, Λ=450, cD=10.81,cE=-0.29,cE1=-4,cE7=0
SMS on: 3NF N2LO, Λ=450, cD=6.97,cE=0.20,cE1=-2,cE7=0
pd 250 MeV Hatanaka
SMS on: 3NF N2LO, Λ=450, cD=-3.13,cE=0.04,cE1=2,cE7=0
SMS on: 3NF N2LO, Λ=450, cD=-11.96,cE=-0.96,cE1=4,cE7=0

SMS: o0 n4lo+, Λ=450 MeV
SMS on: NN N4LO+ 3NF N2LO, Λ=450 MeV, cD=2.7411,cE=0.3671,cE1=cE7=0.0
SMS on: NN N4LO+ 3NF N2LO, Λ=450 MeV, cD=10.471,cE=1.0794,cE1=0,cE7=-4
SMS on: NN N4LO+ 3NF N2LO, Λ=450 MeV, cD=8.5326,cE=0.9248,cE1=0,cE7=-2
pd 250 MeV Hatanaka
SMS on: NN N4LO+ 3NF N2LO, Λ=450 MeV, cD=-8.2053,cE=-1.0019,cE1=0,cE7=2

band o0 (CDBonn,AV18,Nijm1,Nijm2)
band on (CDBonn,AV18,Nijm1,Nijm2)+TM99
pd 250 MeV Hatanaka
AV18+UIX

(AV18,CDBonn,Nijm1,2) bands
E=250 MeV
d(n,n)d

chiral
E=250 MeV
d(n,n)d

T_{21}

Θ_{cm} [deg]

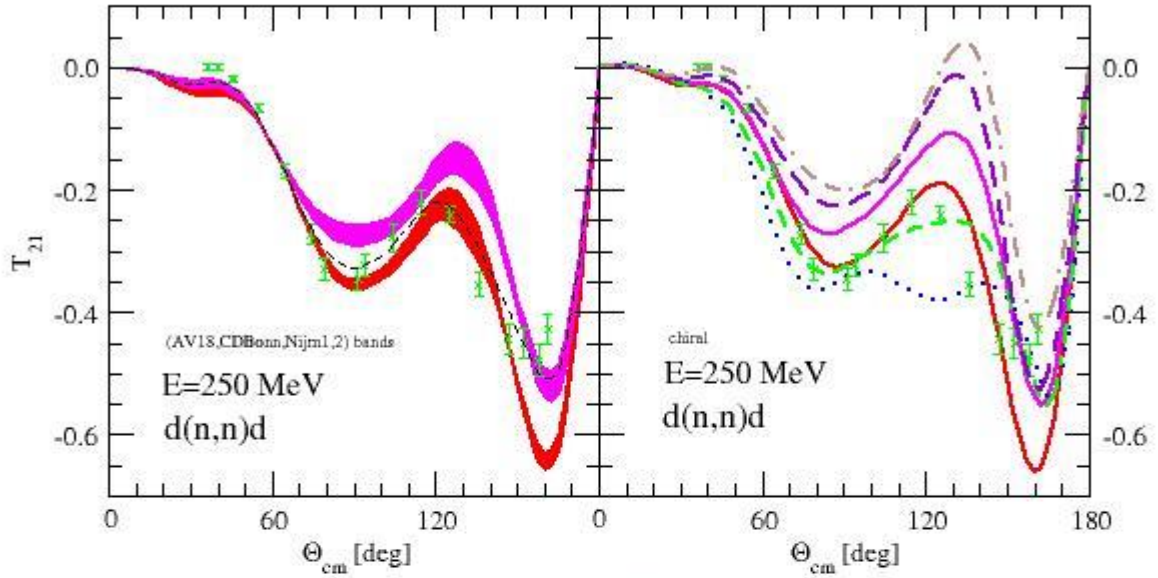

band o0 (CDBonn,AV18,Nijm1,Nijm2)
band on (CDBonn,AV18,Nijm1,Nijm2)+TM99
pd 250 MeV Hatanaka
AV18+UIX

(AV18,CDBonn,Nijm1,2) bands
E=250 MeV
d(n,n)d

chiral
E=250 MeV
d(n,n)d

T_{22}

Θ_{cm} [deg]

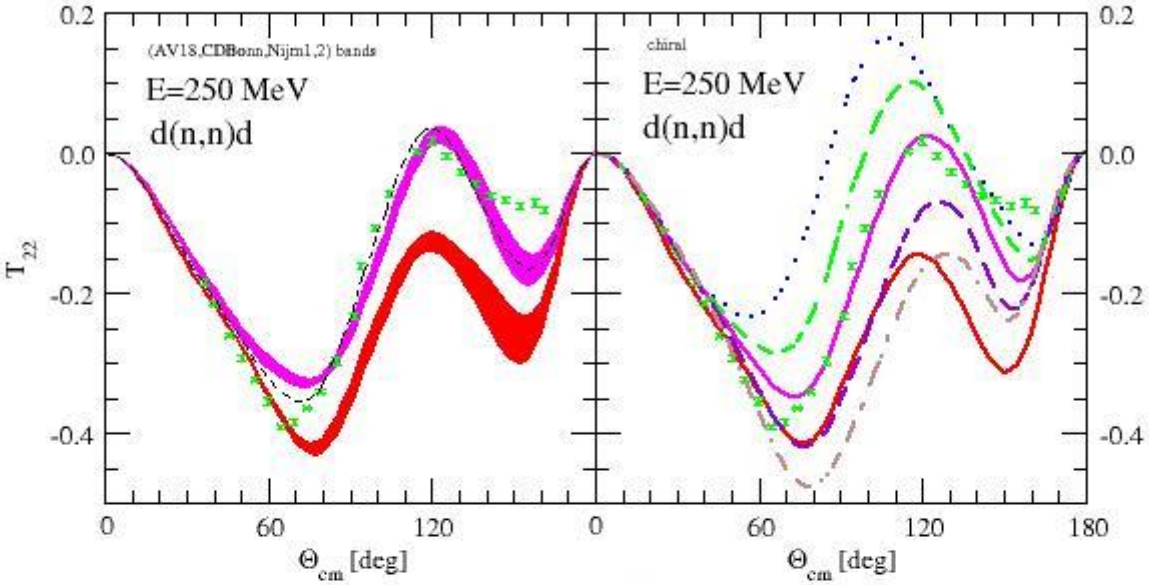

SMS: o0 n4lo+, Λ=450 MeV
SMS on: 3NF N2,4LO, Λ=450, cD=2.74,cE=0.36,cE1=cE7=0.0
SMS on: 3NF N2LO, Λ=450, cD=10.81,cE=-0.29,cE1=-4,cE7=0
SMS on: 3NF N2LO, Λ=450, cD=6.97,cE=0.20,cE1=-2,cE7=0
pd 250 MeV Hatanaka
SMS on: 3NF N2LO, Λ=450, cD=-3.13,cE=0.04,cE1=2,cE7=0
SMS on: 3NF N2LO, Λ=450, cD=-11.96,cE=-0.96,cE1=4,cE7=0

chiral
d(n,n)d
E=250 MeV

T_{21}

Θ_{cm} [deg]

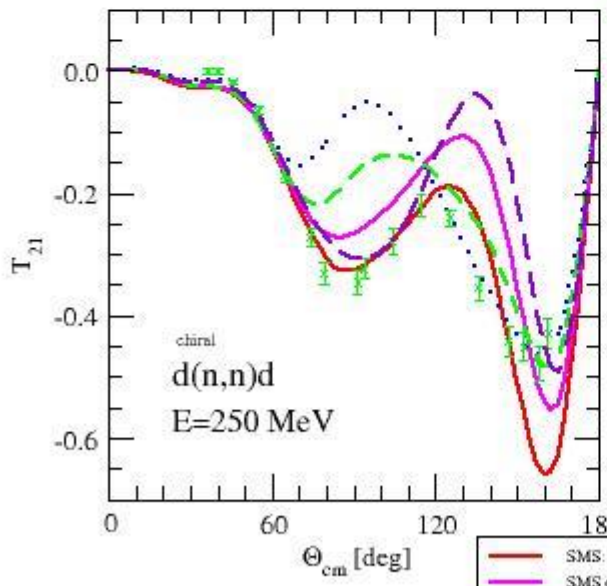

SMS: o0 n4lo+, Λ=450 MeV
SMS on: NN N4LO+ 3NF N2LO, Λ=450 MeV, cD=2.7411,cE=0.3671,cE1=cE7=0.0
SMS on: NN N4LO+ 3NF N2LO, Λ=450 MeV, cD=10.471,cE=1.0794,cE1=0,cE7=-4
SMS on: NN N4LO+ 3NF N2LO, Λ=450 MeV, cD=8.5326,cE=0.9248,cE1=0,cE7=-2
pd 250 MeV Hatanaka
SMS on: NN N4LO+ 3NF N2LO, Λ=450 MeV, cD=-8.2053,cE=-1.0019,cE1=0,cE7=2

SMS: o0 n4lo+, Λ=450 MeV
SMS on: 3NF N2,4LO, Λ=450, cD=2.74,cE=0.36,cE1=cE7=0.0
SMS on: 3NF N2LO, Λ=450, cD=10.81,cE=-0.29,cE1=-4,cE7=0
SMS on: 3NF N2LO, Λ=450, cD=6.97,cE=0.20,cE1=-2,cE7=0
pd 250 MeV Hatanaka
SMS on: 3NF N2LO, Λ=450, cD=-3.13,cE=0.04,cE1=2,cE7=0
SMS on: 3NF N2LO, Λ=450, cD=-11.96,cE=-0.96,cE1=4,cE7=0

chiral
d(n,n)d
E=250 MeV

T_{22}

Θ_{cm} [deg]

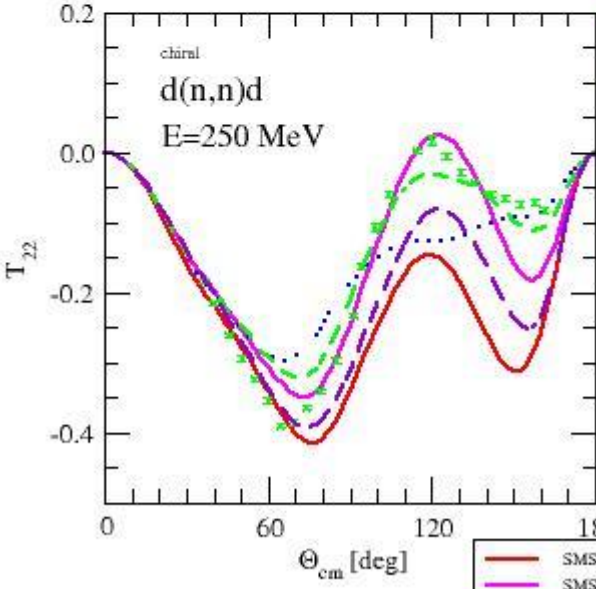

SMS: o0 n4lo+, Λ=450 MeV
SMS on: NN N4LO+ 3NF N2LO, Λ=450 MeV, cD=2.7411,cE=0.3671,cE1=cE7=0.0
SMS on: NN N4LO+ 3NF N2LO, Λ=450 MeV, cD=10.471,cE=1.0794,cE1=0,cE7=-4
SMS on: NN N4LO+ 3NF N2LO, Λ=450 MeV, cD=8.5326,cE=0.9248,cE1=0,cE7=-2
pd 250 MeV Hatanaka
SMS on: NN N4LO+ 3NF N2LO, Λ=450 MeV, cD=-8.2053,cE=-1.0019,cE1=0,cE7=2

band o0 (CDBonn,AV18,Nijm1,Nijm2)
band on (CDBonn,AV18,Nijm1,Nijm2)+TM99
RIKEN 190 MeV pd data
AV18+UIX

(AV18,CDBonn,Nijm1,2) bands
E=190 MeV
d(n,n)d

chiral
E=190 MeV
d(n,n)d

T_{20}

Θ_{cm} [deg]

band o0 (CDBonn,AV18,Nijm1,Nijm2)
band on (CDBonn,AV18,Nijm1,Nijm2)+TM99
pd 250 MeV Hatanaka
AV18+UIX

(AV18,CDBonn,Nijm1,2) bands
E=250 MeV
d(n,n)d

chiral
E=250 MeV
d(n,n)d

T_{20}

Θ_{cm} [deg]

SMS: o0 n4lo+, Λ=450 MeV
SMS on: 3NF N2,4LO, Λ=450, cD=2.74,cE=0.36,cE1=cE7=0.0
SMS on: 3NF N2LO, Λ=450, cD=10.81,cE=-0.29,cE1=-4,cE7=0
SMS on: 3NF N2LO, Λ=450, cD=6.97,cE=0.20,cE1=-2,cE7=0
RIKEN 190 MeV pd data
SMS on: 3NF N2LO, Λ=450, cD=-3.13,cE=0.04,cE1=2,cE7=0
SMS on: 3NF N2LO, Λ=450, cD=-11.96,cE=-0.96,cE1=4,cE7=0

chiral
E=190 MeV
d(n,n)d

T_{20}

Θ_{cm} [deg]

SMS: o0 n4lo+, Λ=450 MeV
SMS on: NN N4LO+ 3NF N2LO, Λ=450 MeV, cD=2.7411,cE=0.3671,cE1=cE7=0.0
SMS on: NN N4LO+ 3NF N2LO, Λ=450 MeV, cD=10.471,cE=1.0794,cE1=0,cE7=-4
SMS on: NN N4LO+ 3NF N2LO, Λ=450 MeV, cD=8.5326,cE=0.9248,cE1=0,cE7=-2
RIKEN 190 MeV pd data
SMS on: NN N4LO+ 3NF N2LO, Λ=450 MeV, cD=-8.2053,cE=-1.0019,cE1=0,cE7=2

SMS: o0 n4lo+, Λ=450 MeV
SMS on: 3NF N2,4LO, Λ=450, cD=2.74,cE=0.36,cE1=cE7=0.0
SMS on: 3NF N2LO, Λ=450, cD=10.81,cE=-0.29,cE1=-4,cE7=0
SMS on: 3NF N2LO, Λ=450, cD=6.97,cE=0.20,cE1=-2,cE7=0
pd 250 MeV Hatanaka
SMS on: 3NF N2LO, Λ=450, cD=-3.13,cE=0.04,cE1=2,cE7=0
SMS on: 3NF N2LO, Λ=450, cD=-11.96,cE=-0.96,cE1=4,cE7=0

chiral
E=250 MeV
d(n,n)d

T_{20}

Θ_{cm} [deg]

SMS: o0 n4lo+, Λ=450 MeV
SMS on: NN N4LO+ 3NF N2LO, Λ=450 MeV, cD=2.7411,cE=0.3671,cE1=cE7=0.0
SMS on: NN N4LO+ 3NF N2LO, Λ=450 MeV, cD=10.471,cE=1.0794,cE1=0,cE7=-4
SMS on: NN N4LO+ 3NF N2LO, Λ=450 MeV, cD=8.5326,cE=0.9248,cE1=0,cE7=-2
pd 250 MeV Hatanaka
SMS on: NN N4LO+ 3NF N2LO, Λ=450 MeV, cD=-8.2053,cE=-1.0019,cE1=0,cE7=2

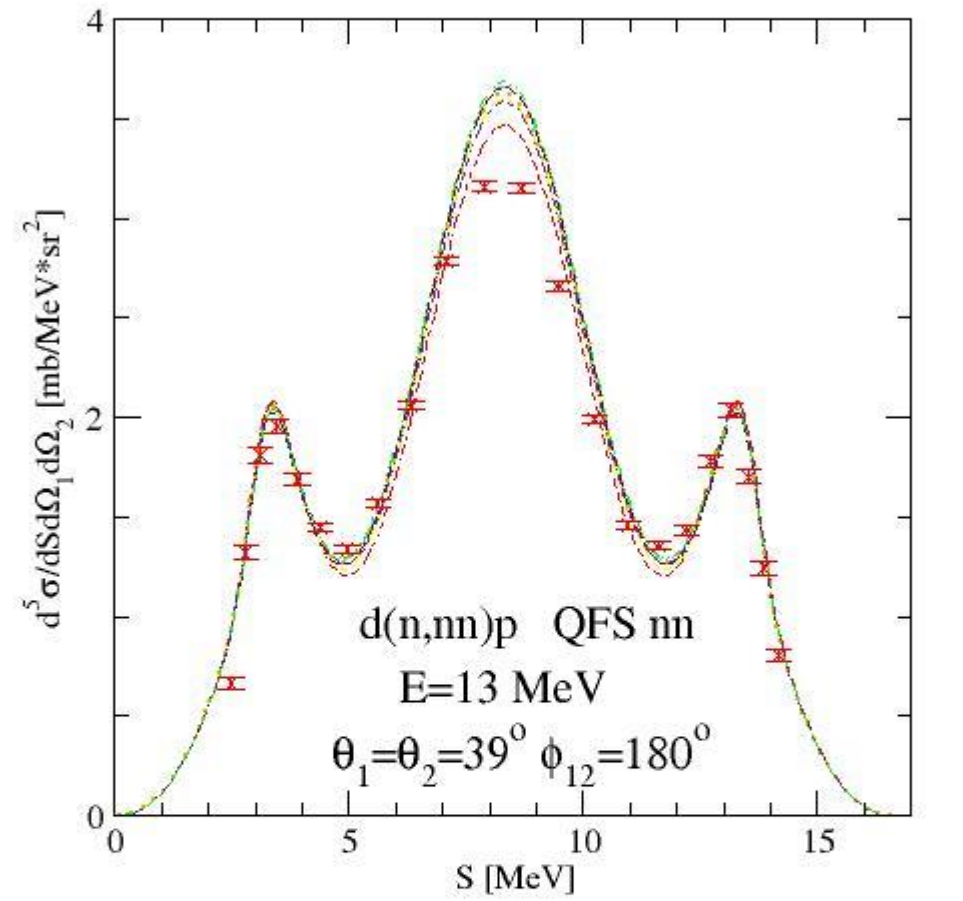

o0: SRS NN N4LO R=0.9 rule ppnp
o0: SMS A=450 NN N4LO+ rule ppnp
on: SMS NN N4LO+ 3NF N2LO+N4LO: cD=2.7411, cE=0.3671, cE1=0.0, cE7=0.0
on: SMS NN N4LO+ 3NF N2LO+N4LO: cD=10.8183, cE=-0.2946, cE1=-4.0, cE7=0.0
on: SMS NN N4LO+ 3NF N2LO+N4LO: cD=-11.9665, cE=-0.9686, cE1=4.0, cE7=0.0
on: SMS NN N4LO+ 3NF N2LO+N4LO: cD=7.8895, cE=-0.8733, cE1=0.0, cE7=-4.0
on: SMS NN N4LO+ 3NF N2LO+N4LO: cD=-8.0638, cE=--1.0068, cE1=0.0, cE7=4.0
Koeln pd data

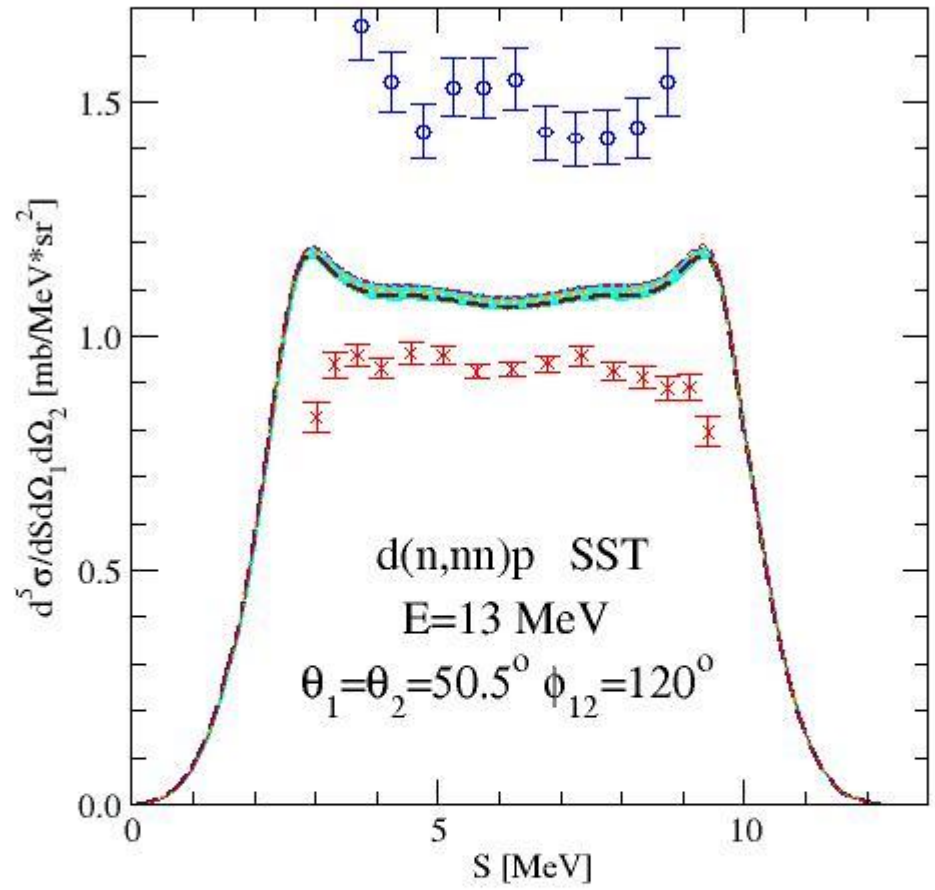

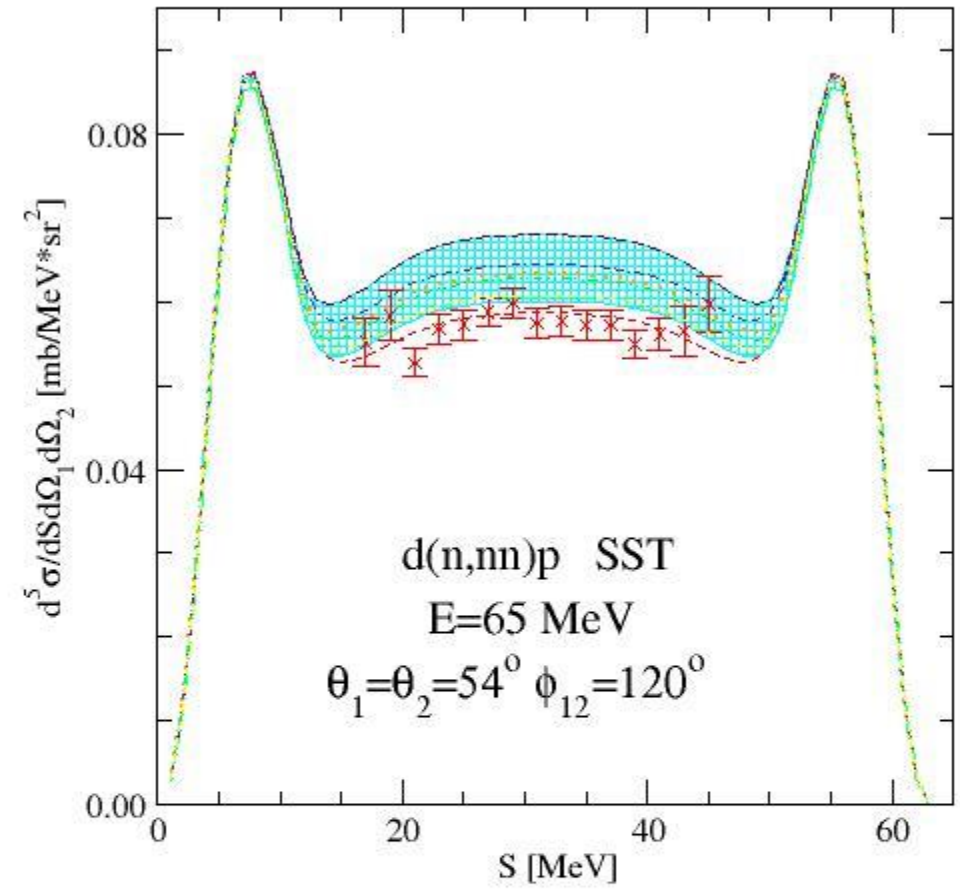

on: band of predictions for 8 combinations of cE1 and cE7
o0: SMS Λ=450 NN N4LO+ rule ppnp
on: SMS NN N4LO+ 3NF N2LO+N4LO: cD=2.7411, cE=0.3671, cE1=0.0, cE7=0.0
TUNL nd data
on: SMS NN N4LO+ 3NF N2LO+N4LO: cD=10.8183, cE=-0.2946, cE1=-4.0, cE7=0.0
on: SMS NN N4LO+ 3NF N2LO+N4LO: cD=-11.9665, cE=-0.9686, cE1=4.0, cE7=0.0
on: SMS NN N4LO+ 3NF N2LO+N4LO: cD=10.471, cE=1.0794, cE1=0.0, cE7=-4.0
on: SMS NN N4LO+ 3NF N2LO+N4LO: cD=-8.2053 cE=--1.0019, cE1=0.0, cE7=2.0
Koeln pd data
o0: SRS NN N4LO R=0.9 rule ppnp

o0: SRS NN N4LO R=0.9 rule ppnp
on: SMS NN N4LO+ 3NF N2LO+N4LO: band for 8 combinations of cE1 and cE7
on: SMS NN N4LO+ 3NF N2LO+N4LO: cD=2.7411, cE=0.3671, cE1=0.0, cE7=0.0
on: SMS NN N4LO+ 3NF N2LO+N4LO: cD=10.8183, cE=-0.2946, cE1=-4.0, cE7=0.0
on: SMS NN N4LO+ 3NF N2LO+N4LO: cD=-11.9665, cE=-0.9686, cE1=4.0, cE7=0.0
on: SMS NN N4LO+ 3NF N2LO+N4LO: cD=10.471, cE=1.0794, cE1=0.0, cE7=-4.0
on: SMS NN N4LO+ 3NF N2LO+N4LO: cD=-8.2053, cE=--1.0019, cE1=0.0, cE7=2.0
Koeln pd data
o0: SMS Λ=450 NN N4LO+ rule ppnp

Conclusion:

The subleading contact 3NF have a potential to resolve the observed discrepancies in Nd scattering between theory and data. In particular, they can increase the differential cross section at backward angles and generate lots of structure in polarization observables seen in the data. (Of course, the inclusion of the long- and intermediate-range contributions to the 3NF will change the pictures.)

Summary:

- Nd elastic scattering and deuteron breakup reaction reveal large sensitivity to underlying nuclear forces --> good tools to test nuclear Hamiltonian
- it is clear, that based on the present day NN forces additional term in nuclear Hamiltonian is needed --> 3NF
- call for consistency between 2N and 3N forces: support and guidance --> chiral perturbation theory approach
- Big challenge: application of chiral N^3LO and N^4LO forces (2- and 3-body) to 3N continuum (especially at higher energies)
- Big challenge (after establishing forces): application of consistent forces and electro-weak currents to different reactions induced by electro-weak probes on 3N bound (^{3}H and ^{3}He) systems
- Final goal: explanation of standard nuclear physics phenomena by chiral dynamics